1. INTRODUCTION

1.1. Historical perspective

The casting of metals is a prehistoric technology. Even though it is not exactly known when casting began, archeologists give the name “chalcolithic” to the period in which the making and use of metals were first being mastered in the Near East and date this period to approximately between 5000 and 3000 BC (i.e. immediately preceding the Bronze Age). The first metal used for casting was native copper as was deduced from chemical analyses of the earliest cast axes and other objects. The fuel employed was charcoal, which supplied a reducing atmosphere when the fire was enclosed in an attempt to reduce the loss of heat and the molds were made of stone of a smooth texture such as steatite or andesite [1].

In the early 1970’s, thixotropic behaviour was discovered in semi-solid metal alloys which lead to the development of thixocasting and rheocasting (collectively called semi-solid metal processing) [2]. Given the long history of metal casting, it can be seen that this new processing technique is a modern technology.

1.2. Heat treatment and age hardening of Al-alloys

Alfred Wilm accidentally discovered age hardening in an Al-Cu-Mg alloy only approximately 100 years ago and thereby paved the way for using Al-alloys as engineering materials [3]. It took another 30 years before the mechanism of age-hardening could be explained, when in 1938, Guinier and Preston postulated that small precipitates were responsible for the effect [4,5].

1.2.1. Al-Si-Mg alloys

The commercial attraction of Al-Si cast alloys is based on the discovery of modification of the Al-Si eutectic around 1920 by Aladar Pacz [6]. He discovered that the brittle Al-Si eutectic changed its morphology from long plates to fine acicular fibres when small quantities of alkali fluoride or sodium or potassium were added to the melt. In 1921, Al-Si alloys containing up to 15% silicon were introduced in the United States under the trade name "ALPAX" [7]. After World War I, Germany could not afford to use copper in its aluminium alloys and the Al-Si castings provided an alternative for example in the motor blocks of the Daimler cars. The alloy was also used in France in streetcars and railways [6].

The addition of magnesium to Al-Si alloys makes them age-hardenable and these alloys were also developed in the 1920's [8]. The yield strengths of Al-Si-Mg alloys in the T6 condition are more than double that of the binary Al-Si alloys containing the same quantity of Si. They also exhibit good corrosion resistance and are used in the aerospace and automotive industries [9]. With the advent of semi-solid metal (SSM) processing, the Al-7Si-Mg alloys soon became the most popular alloys for study [10]. This is due to their good castability and fluidity imparted by the large volumes of the Al-Si eutectic, with the additional advantage of the castings being age-hardenable to improve strength.

1.3. Heat treatment of Al-7Si-Mg alloys

1.3.1. Conventional liquid cast Al-7Si-Mg alloys

Rinderer and co-workers [11] lamented the lack of detailed research work revealing precipitate micro- and nanostructural evolution during aging of the Al-Si-Mg casting alloys as recently as 2010. They attributed this situation to difficulties the eutectic component causes in preparing high-quality samples for transmission electron microscopy (TEM) and atom probe tomography (APT).

1.3.2. SSM-processed Al-7Si-Mg alloys

Dewhirst [12] stated that: "Due to the differences in thermal history and rheological character between semi solid material and liquid metal, the necessary processing steps are not the same as they have been for thousands of years of foundry experience. The intuition of foundrymen, developed as the trade itself did over the millennia, is not necessarily correct when it comes to semi solid metallurgy. Although knowledge of the mechanisms behind heat treatment of metals is not nearly as old as metal casting itself, those mechanisms have been around for almost 100 years. Through forging, heat treatments have been around in one fashion or another for much longer. As with all new processes, after the mechanisms for SSM heat treatment were commercialised, the first heat treatments applied to it were essentially those already in use for dendritic (liquid cast) materials. These treatment regimes are not necessarily the optimal ones, as the differing microstructure and solidification history of SSM components changes a number of factors." He continued that: "The heat treatment principles for conventionally cast aluminum alloys are well understood, but the different microstructure and solidification history of SSM components indicate that heat

treatment conditions which were optimised for conventionally cast materials do not apply to SSM components."

However, Birol [13,14] postulated that the morphology of the primary α-Al, whether dendritic or globular, has no effect on the artificial aging response of Al-7Si-Mg alloys. He suggested that the favourable impact of the globular structure is most likely offset by the relatively coarser structure in SSM-processed alloys. There is, therefore, disagreement regarding the effects of SSM-processing on the subsequent heat treatment response of these alloys.

1.4. Objective

The objective of this study is to characterise the heat treatment response of SSM-processed Al-7Si-Mg alloys in comparison with conventionally liquid cast alloys (investment casting and gravity die casting). The heat treatment parameters that are specified for conventionally liquid cast alloys are critically analysed to determine whether they are applicable to SSM-processed components and if they are still the same optimised parameters for dendritic castings in a world where energy and environmental features have changed since these cycles were originally developed.

The investigated heat treatment cycles include parameters that affect the T4, T5 and T6 temper conditions i.e. the effects of solution heat treatment, quenching, natural aging and artificial aging on hardness, tensile properties and impact properties are considered. Chemical composition variations within specification (especially Mg) also constitute a major part of this study. Techniques such as optical microscopy, scanning electron microscopy, transmission electron microscopy and atom probe tomography were employed to obtain an in-depth understanding of the processes that occur during heat treatment of these alloys. In addition, commercially available software packages Thermo-Calc and ProCAST were used to supplement the experimental observations. Finally, an age-hardening model was developed based on the Shercliff and Ashby methodology [15], including a method of incorporating the effects of changes in Mg-content on the aging curves.

1.5. Publications

During the course of this study, a number of papers relating to the investigation have been authored or co-authored by Heinrich Möller. These papers are distinguished from other papers by including “HM” in front of the number in the reference list [HM1-HM15].

2. LITERATURE SURVEY

2.1. Semi-solid metal processing

2.1.1. History and introduction

Thixotropy can be derived from the Greek words for “contact, touch”, and “change, modification” [6]. Thixotropic materials flow when sheared, but when allowed to stand they thicken up again. Common materials that display this behaviour are mascara, honey and certain kinds of paint [16]. Thixotropic behaviour in metallic alloys was first discovered by Spencer and co-workers in the early 1970’s while they worked on hot tearing in the lead-tin system [2]. It was found that stirring the metal alloys continuously during cooling from the fully liquid state to the semi-solid state lowered the viscosity significantly compared to when the alloy was cooled into the semi-solid state without stirring. Stirring breaks up the dendrites which would be present in conventionally liquid cast alloys and results in a microstructure in the semi-solid state consisting of spheroids or globules of solids surrounded by liquid (Fig. 2.1 [17]).

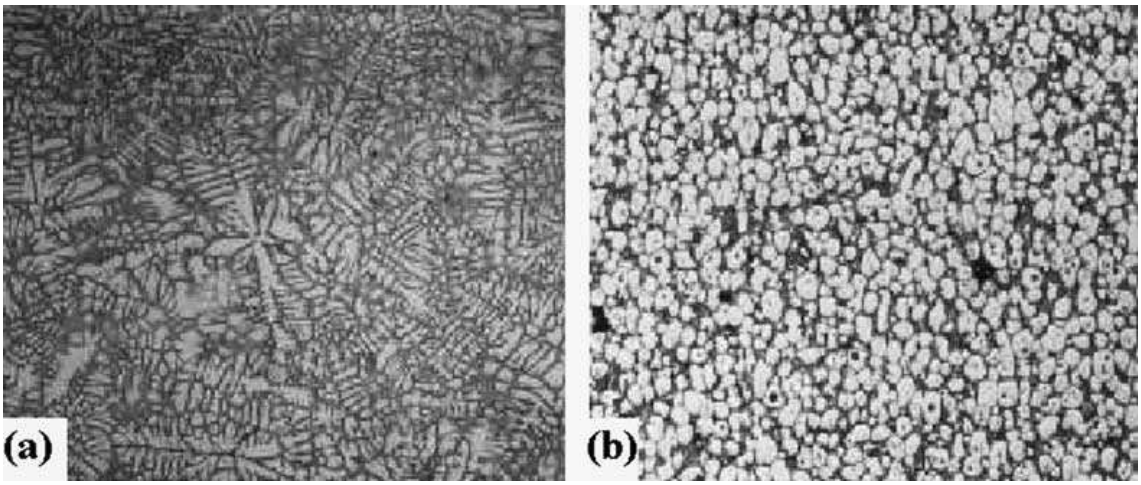

Figure 2.1: Micrograph of a typical (a) dendritic microstructure in an as-cast sample and (b) globular microstructure in a semi-solid alloy sample [16].

This globular microstructure is a prerequisite for thixotropic behaviour and when such a semi-solid microstructure is allowed to stand, the globules/spheroids agglomerate and the viscosity increases with time [16]. If the material is sheared, the agglomerates are broken up and the viscosity decreases. In the semi-solid state (with ~ 30-50% liquid), the alloy will support its own weight when allowed to stand and can be handled as a solid. However, as soon as it is sheared, it flows with a viscosity similar to that of heavy machine oil. The cutting test, in which the alloy can be cut and spread

like butter, demonstrates the thixotropic behaviour of semi-solid alloy slugs in Figure 2.2 [16].

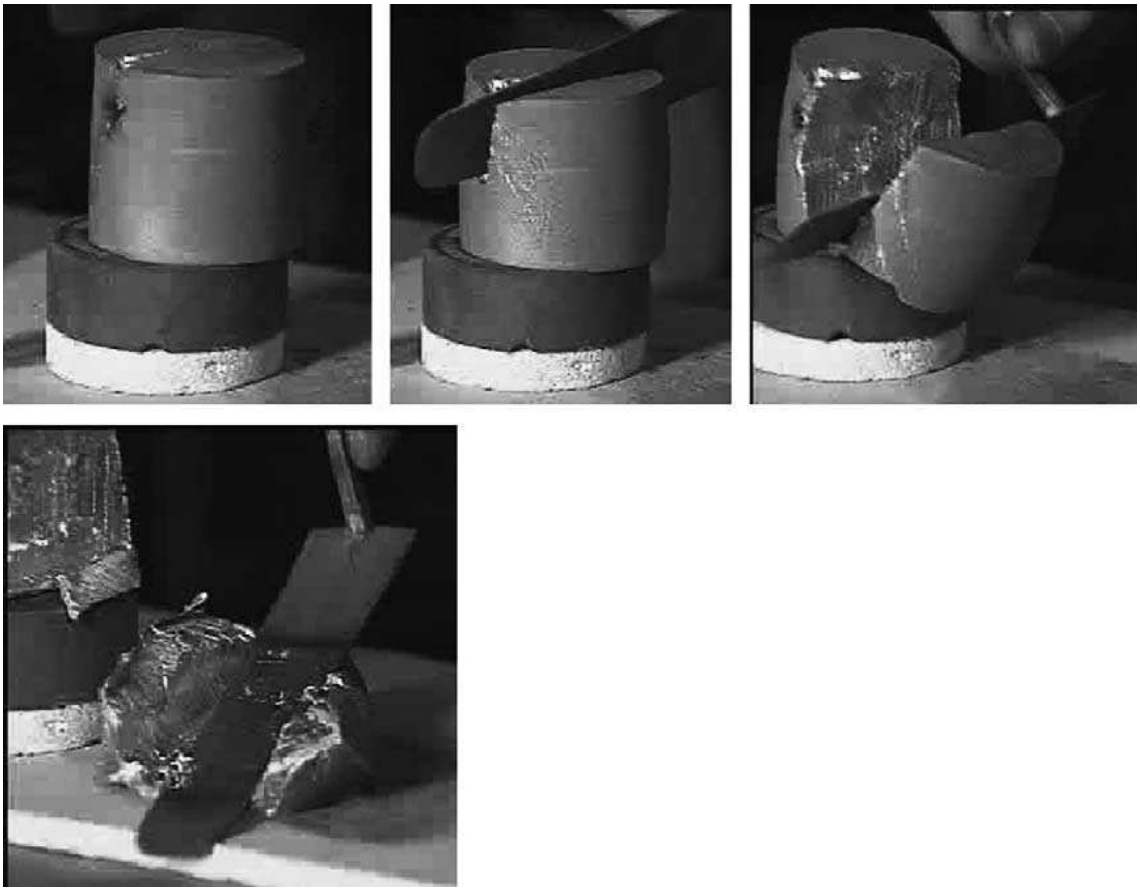

Figure 2.2: A photographic sequence illustrating the thixotropic behaviour of semi-solid alloy slugs [16].

More than 30 years of research has been invested in the field of SSM-processing and the interest in the field is highlighted by eleven international conferences [17-27] with a twelfth planned in South Africa in 2012. SSM-processing presents an alternative manufacturing route for aerospace, military and especially automotive components [16,28]. Suspension parts, engine brackets and fuel rails for automotives are being produced in Europe, whereas examples from the USA include mechanical parts for snowmobiles and mountain bikes. Asia has focused more on the production of electronic components such as electrical housing components and notebook cases with emphasis on magnesium alloys [16]. Two main routes have subsequently been developed for producing semi-solid parts, namely thixoforming and rheocasting.

2.1.2. Thixoforming

Thixoforming is a general term used to describe the near-net shape forming processes from a partially melted, non-dendritic alloy slug within a metal die. If the component shaping is performed in a closed die, it is referred to as thixocasting, while if the shaping is achieved in an open die, it is called thixoforging [6,16]. There are two separate stages involved in the thixoforming process namely reheating and forming. Reheating to the semi-solid state is a particularly important phase in the thixoforming process and is mainly achieved by induction heating, which guarantees exact and rapid heating. The increased costs associated with thixocasting (for example recycling of thixocast scrap and the necessity of an outside manufacturer for billet production) have resulted in rheocasting becoming the preferred semi-solid process [16].

2.1.3. Rheocasting

Rheocasting involves preparation of a SSM slurry directly from the liquid, followed by a forming process such as high pressure die casting (HPDC). Component shaping directly from SSM slurries is inherently attractive due to its characteristics, such as overall efficiency in production and energy management [6]. The distinctions between thixocasting, thixoforging and rheocasting are illustrated graphically in Figure 2.3 [29].

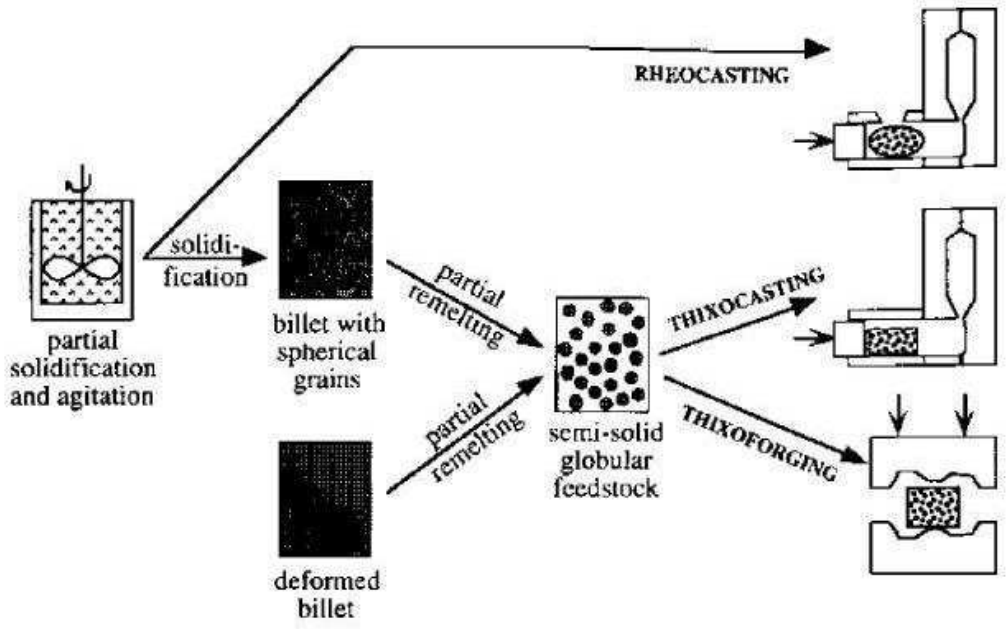

Figure 2.3: Schematic illustration of different routes for SSM-processing [29].

2.1.3.1. CSIR rheocasting system (CSIR-RCS)

The Council for Scientific and Industrial Research (CSIR) in South Africa has developed and patented a rheoprocessing system which uses combined coils for induction stirring and simultaneous forced air cooling, named the CSIR RheoCasting System (CSIR-RCS) [30,31]. One of the features of the equipment and process required that it be flexible so that it could be used on both horizontal and vertical injection high pressure die casting equipment and be implemented in most existing HPDC foundries without significant capital investment. It also has to be able to produce a billet per minute with the ability to vary the cycle time as needed. Using these requirements, the equipment for treatment of light metal alloys from liquid state to semi-solid slurry (Figure 2.4) was developed. Cups filled with metal move in a vertical direction upwards and stepwise through three conditioning units. Each conditioning unit consists of an induction coil and air-cooling. The equipment can be operated as units of a single coil, two coils or three coils depending on the production requirements and material being processed. After rheoprocessing the semi-solid billet is transferred to a HPDC machine for casting.

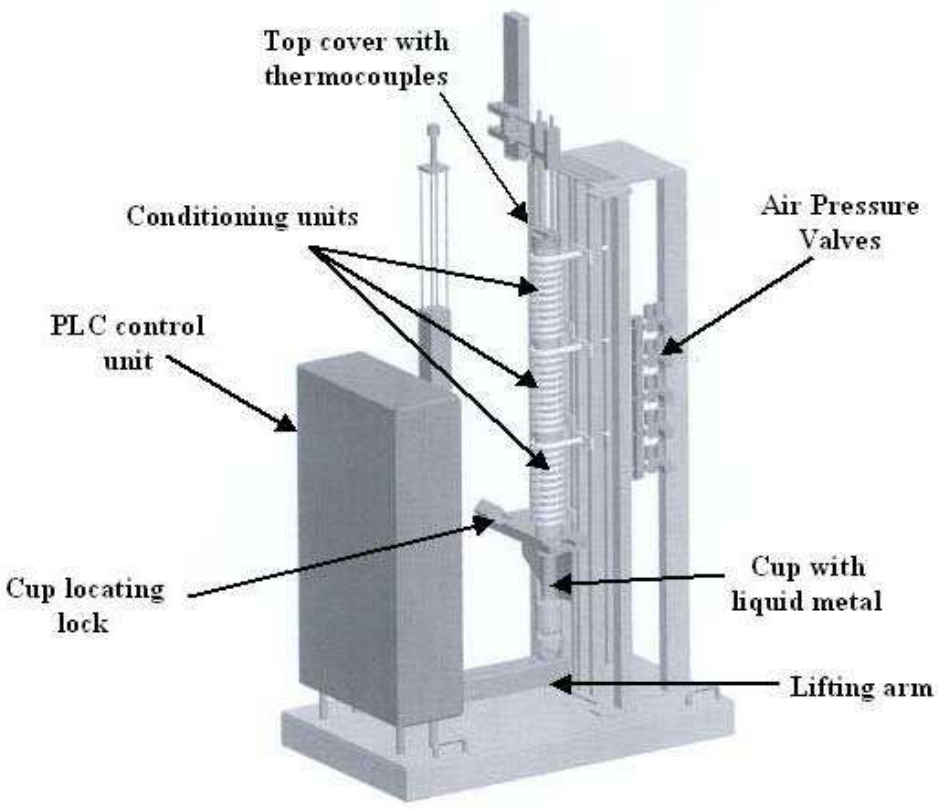

Figure 2.4: The CSIR Rheoprocessing slurry maker for continuous delivery of SSM billets [31].

2.1.4. Advantages and disadvantages of SSM-processing

The main advantages and disadvantages of semi-solid processing (relative to die casting) have been summarised by Atkinson [16] to be as follows:

Advantages

- Energy efficiency: metal is not being held in the liquid state over long periods of time;
- Production rates are similar to pressure die casting or better;
- Smooth filling of the die with no air entrapment and low shrinkage porosity gives parts of high integrity (including thin-walled sections) and allows application of the process to higher-strength heat-treatable alloys;
- Lower processing temperatures reduce the thermal shock on the die, promoting die life and allowing the use of non-traditional die materials;
- Fine, uniform microstructures give enhanced properties;

- Reduced solidification shrinkage gives dimensions closer to near net shape and justifies the elimination of machining steps; and
- Surface quality is suitable for plating.

Disadvantages

- The cost of raw material for thixoforming can be high and the number of suppliers small;
- Process knowledge and experience has to be continually built up in order to facilitate application of the process to new components;
- Initially at least, personnel require a higher level of training and skill than with more traditional processes;
- Temperature control: the fraction solid and viscosity in the semi-solid state are very dependent on temperature. Alloys with a narrow temperature range in the semi-solid region require accurate control of the temperature; and
- Liquid segregation due to non-uniform heating can result in non-uniform composition in the component.

2.2. Al-7Si-Mg alloys

The Al-Si binary alloy system is an eutectic system with the eutectic composition at 12.6wt% Si (Fig. 2.5 [32]).

Conventional casting alloys Al-7Si-Mg A356/7 contain between 6.5 and 7.5% Si, together with 0.25-0.7% Mg and are used for critical castings in aircraft such as the engine support pylons, while automotive components include wheels and cylinder heads [9]. These alloys are probably the most popular alloys used for semi-solid metal forming due to good castability and fluidity imparted by the large volumes of the Al-Si eutectic [10].

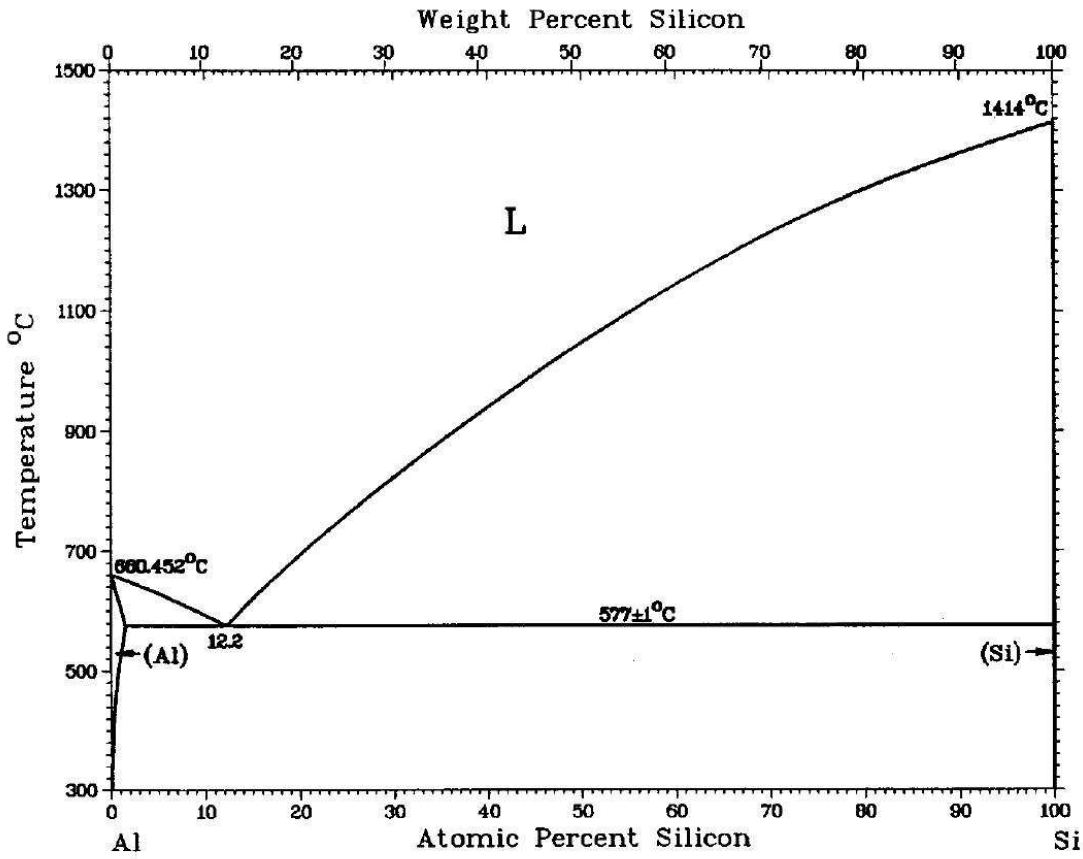

Figure 2.5: The Al-Si binary phase diagram [32].

The chemical composition limits for alloys A356, as well as A357 to F357 are shown in Table 2.1 [33]. International standards for aluminium alloys often permit significant fluctuations in the content of alloying elements. The main difference between alloy A356 and the F357 alloy lies in the magnesium content, whereas the main difference between alloys F357 and A357 is their beryllium content (Table 2.1). The addition of beryllium to this alloy system (e.g. alloy A357) leads to a change in the morphology of the iron-rich intermetallics, which results in slightly better ductility [34] – see section 2.2.1.4. The Be-containing alloys are gradually being phased out in many applications due to the carcinogenic effects of beryllium, particularly at higher concentrations used during make-up of the alloys. The beryllium-free alloy F357 is frequently incorrectly labelled as A357, especially in semi-solid metal research [35,36].

Table 2.1: Chemical composition limits (in wt%) for alloys A356, A357, B357, C357, D357, E357 and F357 [33].

		Si	Mg	Fe	Cu	Mn	Ti	Be
A356	Min	6.5	0.25	-	-	-	-	-
	Max	7.5	0.45	0.20	0.20	0.10	0.20	-
A357	Min	6.5	0.40	-	-	-	0.10	0.04
	Max	7.5	0.70	0.20	0.20	0.10	0.20	0.07
B357	Min	6.5	0.40	-	-	-	0.04	-
	Max	7.5	0.60	0.09	0.05	0.05	0.20	-
C357	Min	6.5	0.45	-	-	-	0.04	0.04
	Max	7.5	0.70	0.09	0.05	0.05	0.20	0.07
D357	Min	6.5	0.55	-	-	-	0.10	0.04
	Max	7.5	0.60	0.20	-	0.10	0.20	0.07
E357	Min	6.5	0.55	-	-	-	0.10	-
	Max	7.5	0.60	0.10	-	0.10	0.20	0.002
F357	Min	6.5	0.40	-	-	-	0.04	-
	Max	7.5	0.70	0.10	0.20	0.10	0.20	0.002

2.2.1. Influence of important alloying elements in modified Al-7Si-Mg alloys

2.2.1.1. Silicon

Silicon promotes castability because of the high fluidity imparted by the presence of large volumes of the Al-Si eutectic and together with magnesium it forms strengthening precipitates during heat treatment [9]. Silicon is a faceted phase and makes the Al-Si eutectic an irregular eutectic. Silicon also reduces the thermal expansion coefficient and increases corrosion and wear resistance. At room temperature, hypoeutectic alloys such as A356/7 consist of a soft and ductile primary α-Al phase and a hard and brittle eutectic phase containing secondary α-Al and silicon (Fig. 2.6 [37]). Silicon has the strongest influence on the ratio of solid to liquid fraction of all alloying elements in A356/7 and a fluctuation of 1 wt% silicon in aluminium (as is allowed according to Table 2.1) results in a solid fraction change of almost 9% if the casting temperature is held constant [38].

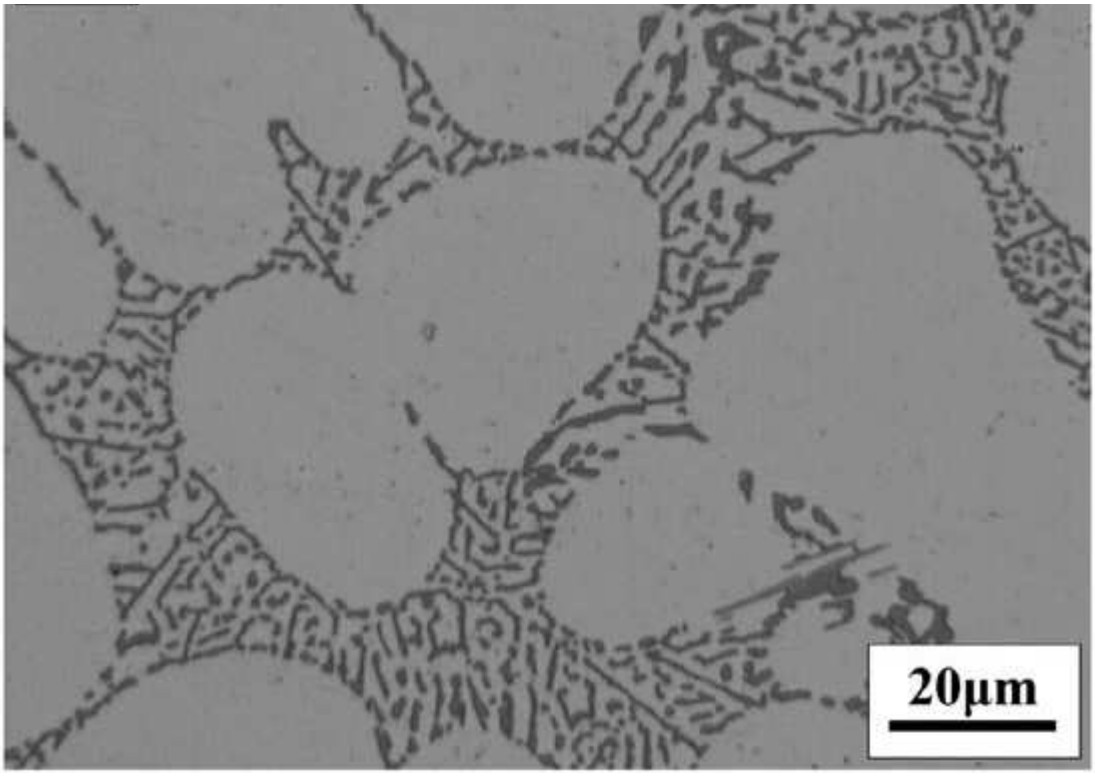

Figure 2.6: Microstructure of alloy A356 showing primary α-Al and the α-Al/Si eutectic [37].

2.2.1.2. Magnesium

Small additions of magnesium induce significant age hardening and the yield strength in the T6 condition has been shown to be more than double that of the binary alloy containing the same amount of silicon [9]. The complete precipitation process in Al-Si-Mg alloys is acknowledged as possibly being the most complex of all age-hardened aluminium alloys [9]. For these alloys in general, the decomposition of the supersaturated solid solution (SSS) is believed to occur as shown in equation 2.1 [39-42]:

$$\mathbf{SSS \rightarrow (Mg + Si)_{clusters} / GP\text{-}I_{spherical} \rightarrow \beta'' / GP\text{-}II_{needles} \rightarrow \beta_{rods}' \rightarrow \beta_{plates} \ (+ Si)} \qquad \mathbf{(2.1)}$$

- GP = Guinier-Preston zones which are spherical with structures that are not well defined [9]. A high resolution transmission electron micrograph (HRTEM) of a naturally aged Si-excess wrought Al-Mg-Si alloy displays a uniform fringe contrast as shown in Fig. 2.7(a) [43]. No contrast attributed to precipitate

particles is observed. On the other hand, the contrast arising from the precipitate particles is observed in the Si-excess alloy that was pre-aged at 70°C for 16 h. The HRTEM image indicates that the precipitates are approximately 2 nm in size and are coherent with the matrix, and the precipitates were therefore designated as GP zones [43].

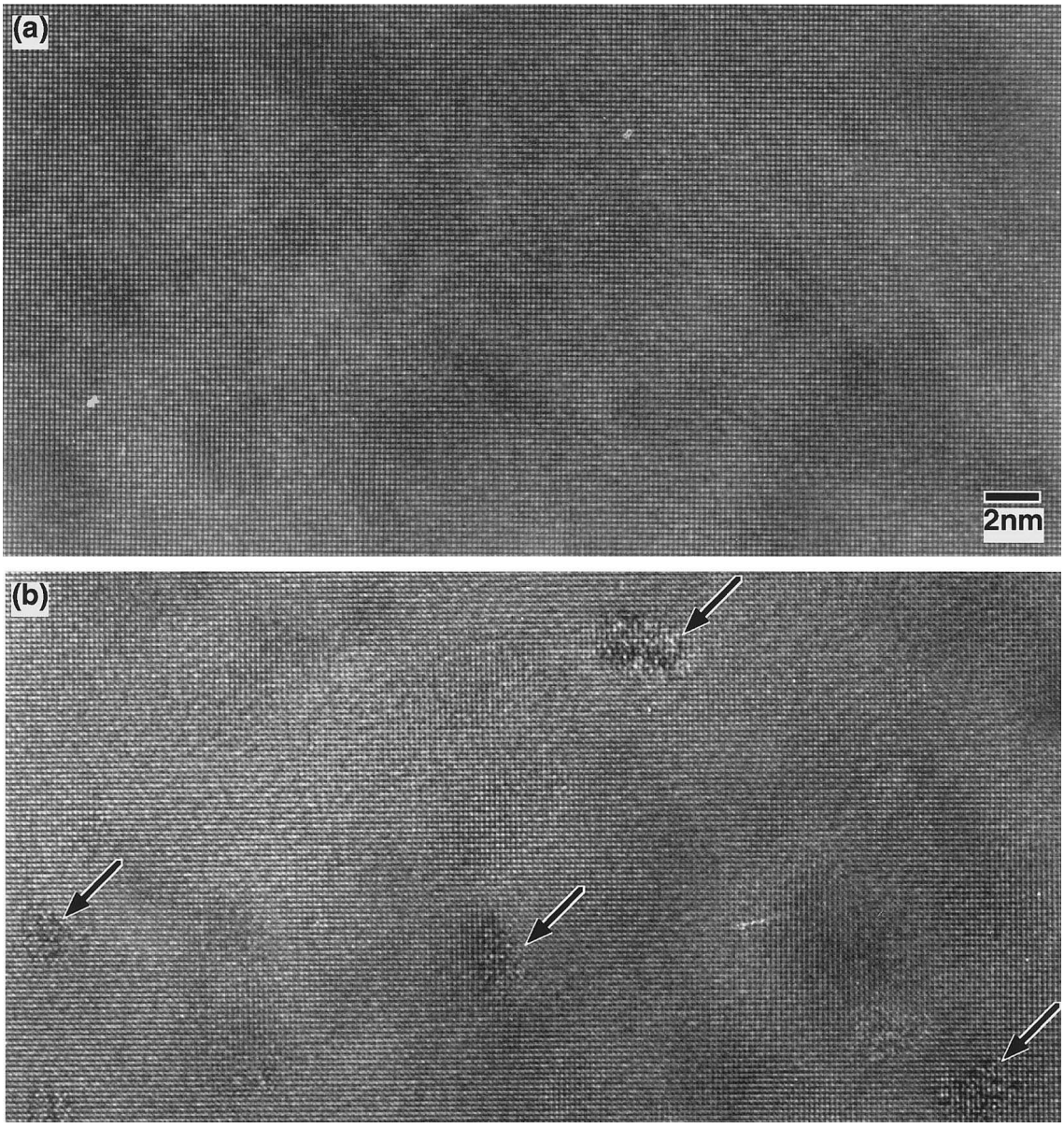

Figure 2.7: HRTEM images taken at the [001]Al zone axis of Al-0.65Mg-0.70Si (Si-excess) alloy after (a) natural aging and (b) 70°C pre-aging [43].

- β″ is a metastable precursor of first β′ and then the stable β. It is monoclinic (three unequal axes with the angles between the axes $\alpha = \gamma = 90^{o} \neq \beta$) with a = 1.534 nm, b = 0.405 nm, c = 0.683 nm and $\beta = 106^{o}$ [9,44]. The β″ precipitates

as coherent needles and lies along $<100>_{\alpha}.(010)_{\beta''}//(001)_{\alpha};[001]_{\beta''}//[310]_{\alpha}$. β″–needles precipitated in alloy A356 aged at 180°C for 2 h are shown in Figure 2.8 [11].

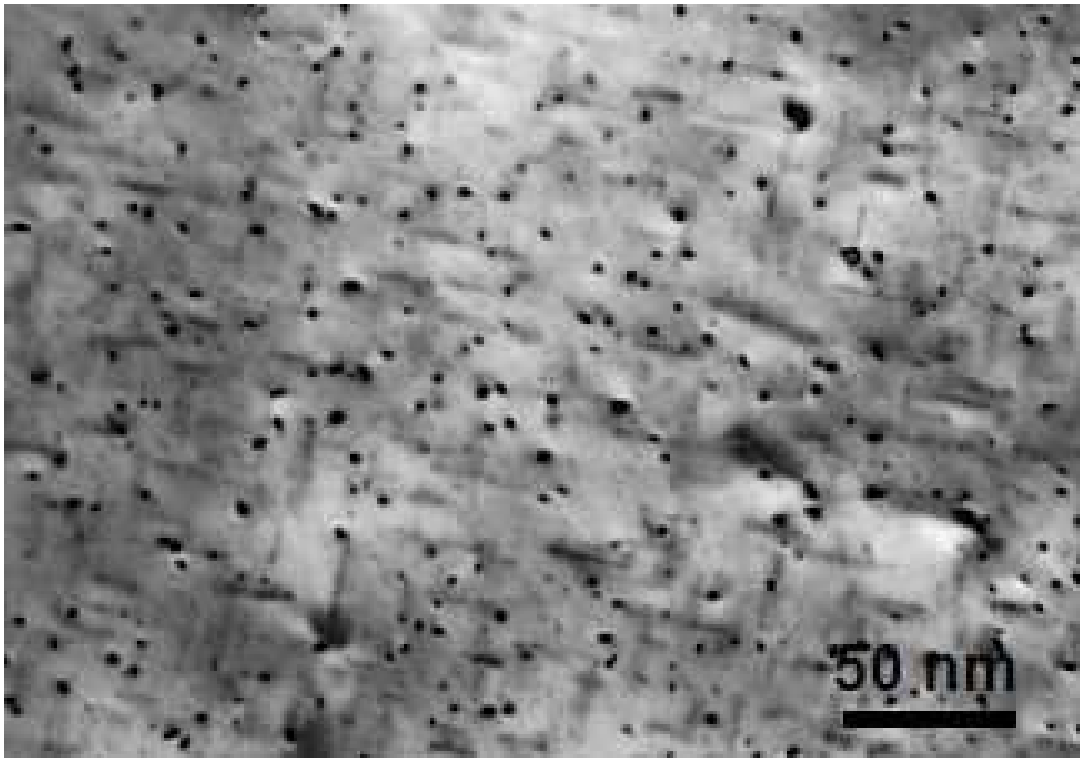

Figure 2.8: TEM image showing β″–needles in an A356 alloy artificially aged at 180°C for 2 h [11].

The β″ precipitate is the main strengthening precipitate in Al-Mg-Si alloys and the composition is thought to be Mg_5Si_6 [45]. However, Buha and co-workers [42] have detected ~ 75 at% Al in these precipitates in the wrought Al-Mg-Si alloy 6061-T6.

- β′ is also a metastable precursor to β with a hexagonal crystal structure with a = 0.705 nm, c = 0.405 nm [9,39]. They precipitate as semi-coherent rods which lie along $<100>_{\alpha}.(001)_{\beta'}//(100)_{\alpha};[100]_{\beta'}//[011]_{\alpha}$ (Fig 2.9 [39]). The composition is believed to be close to $Mg_{1.7}Si$ [9].

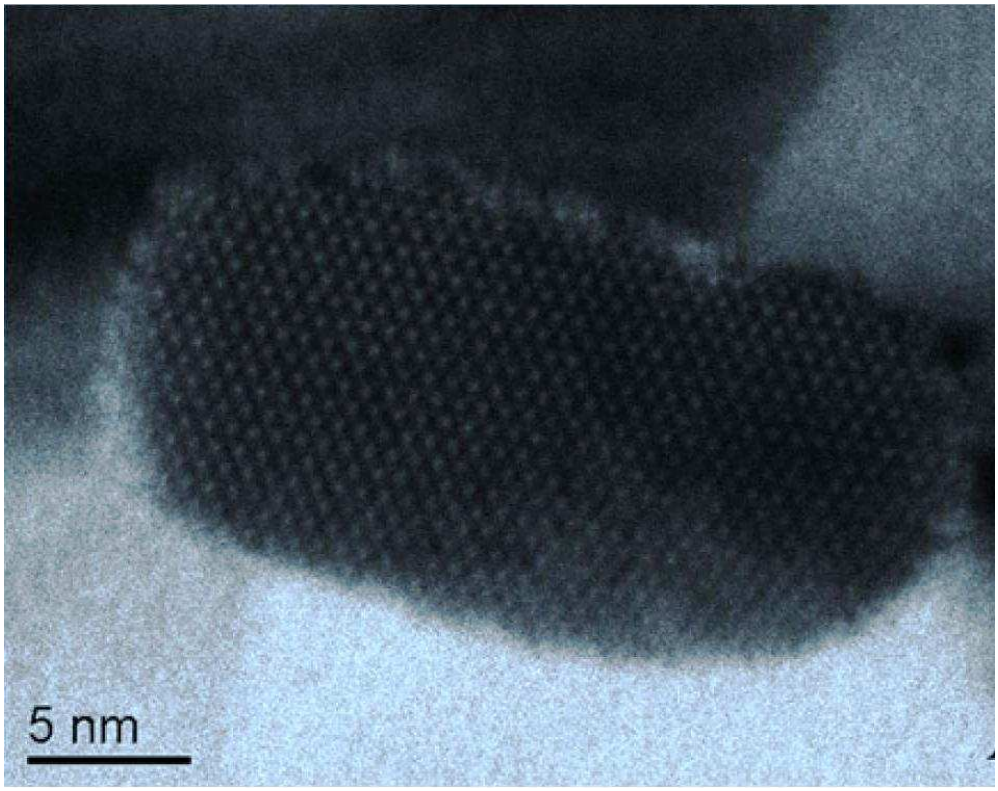

Figure 2.9: HRTEM image showing a β′–rod in a wrought 6082 alloy artificially aged at 260°C for 8 h [39].

- β = Equilibrium Mg_2Si which is face-centred cubic with a = 0.639 nm [9]. The plates or cubes are formed on $\{100\}_\alpha$. They may transform directly from β′ with $(100)_\beta$// $(100)_\alpha$; $[110]_\beta$//$[100]_\alpha$. Figure 2.10 [46] shows typical morphologies of primary Mg_2Si particles at different growth stages in an Al-15%Mg_2Si alloy.

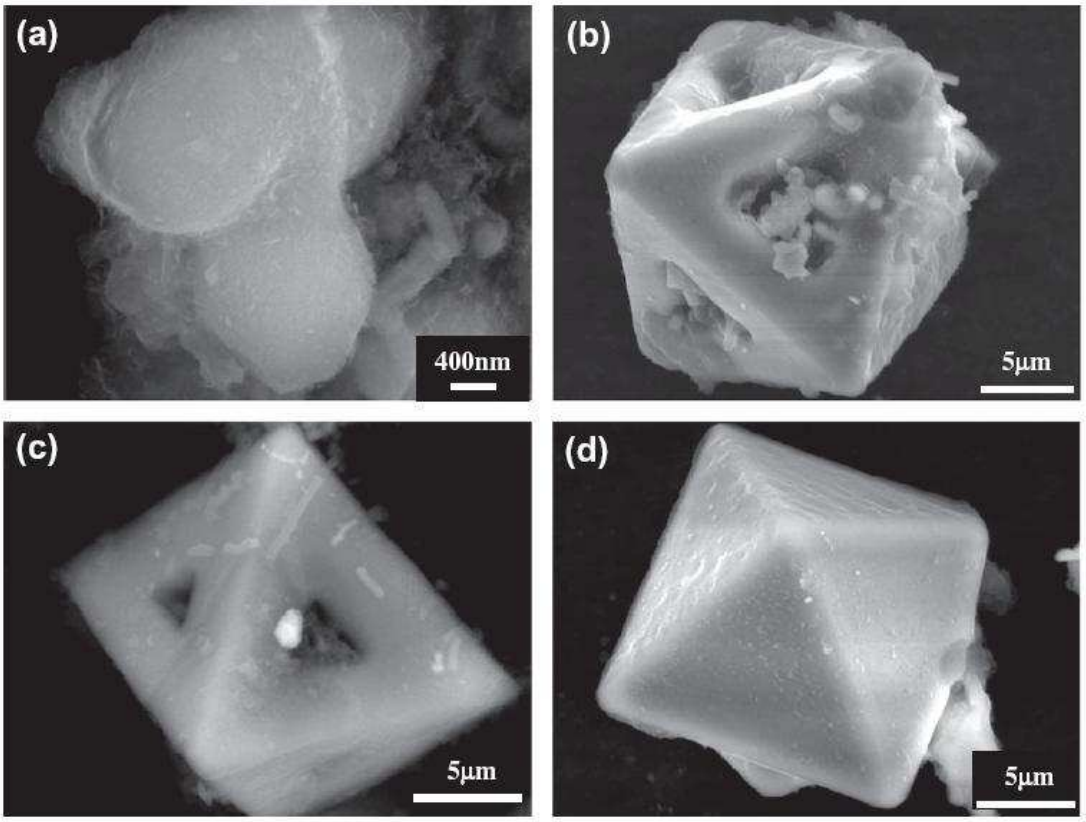

Figure 2.10: Typical morphologies of primary Mg_2Si particles at different growth stages in an Al-15%Mg_2Si alloy [46].

2.2.1.3. Iron

Iron is the most common impurity found in aluminium. It has a high solubility in molten aluminium, but only a maximum of ~ 0.05% in the solid state. Iron, therefore, occurs mainly as intermetallic second phases in combination with aluminium and other elements [33]. Figure 2.11 shows a SEM micrograph of π-$Al_8FeMg_3Si_6$ and β–Al_5FeSi particles in a Be-free alloy F357 [34]. The plate-like phase (indicated as arrow 1) was identified as β–Al_5FeSi, whereas the Chinese script phase (indicated as arrow 2) was identified as π-$Al_8FeMg_3Si_6$. Taylor and co-workers [47,48] have studied the influence of solution treatment on the changes to the relative proportions of iron-containing intermetallic particles in Al-7Si-Mg alloys. They showed that solution treatment caused a substantial transformation of the π-phase ($Al_8FeMg_3Si_6$) to the Mg-free β-phase (Al_5FeSi) in low Mg alloys (0.3-0.4 % or A356). However, this transformation does not occur at higher Mg levels (0.6-0.7% or F357). The transformation of Mg-containing π to β–Al_5FeSi is accompanied by a release of Mg

into the aluminium matrix, which should have an influence on the subsequent aging response of the alloy (equation 2.1).

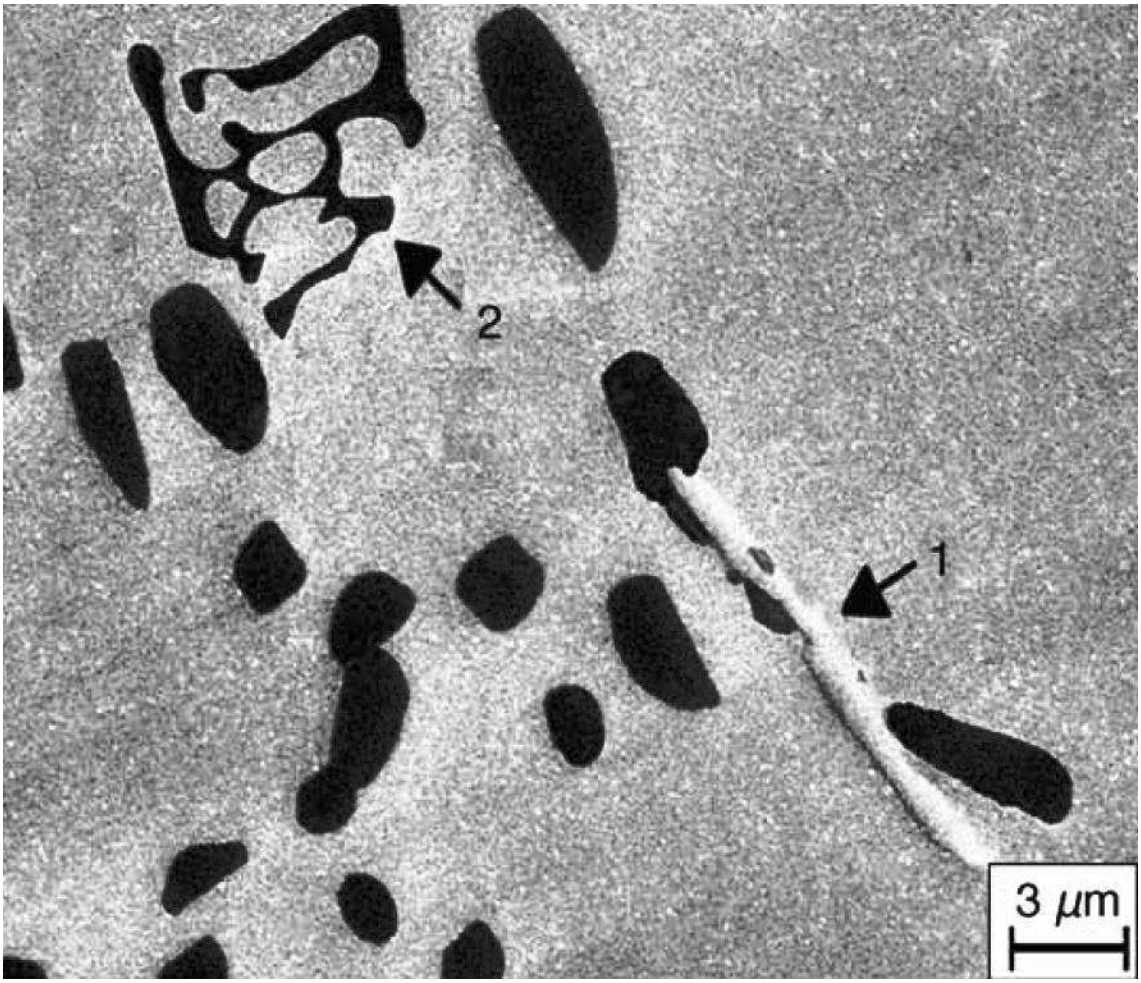

Figure 2.11: SEM micrograph showing the presence of plate-like β–Al_5FeSi (arrow 1) and Chinese-script π-$Al_8FeMg_3Si_6$ (arrow 2) in a Be-free alloy F357 [34].

2.2.1.4. Beryllium

The addition of beryllium to this alloy system leads to a change in the morphology of the iron-rich intermetallics, which results in a slightly better ductility [34]. Figure 2.12 shows that adding Be to the alloy changes the plate-like β–Al_5FeSi phase (Fig. 2.11) to a spherical shape [34].

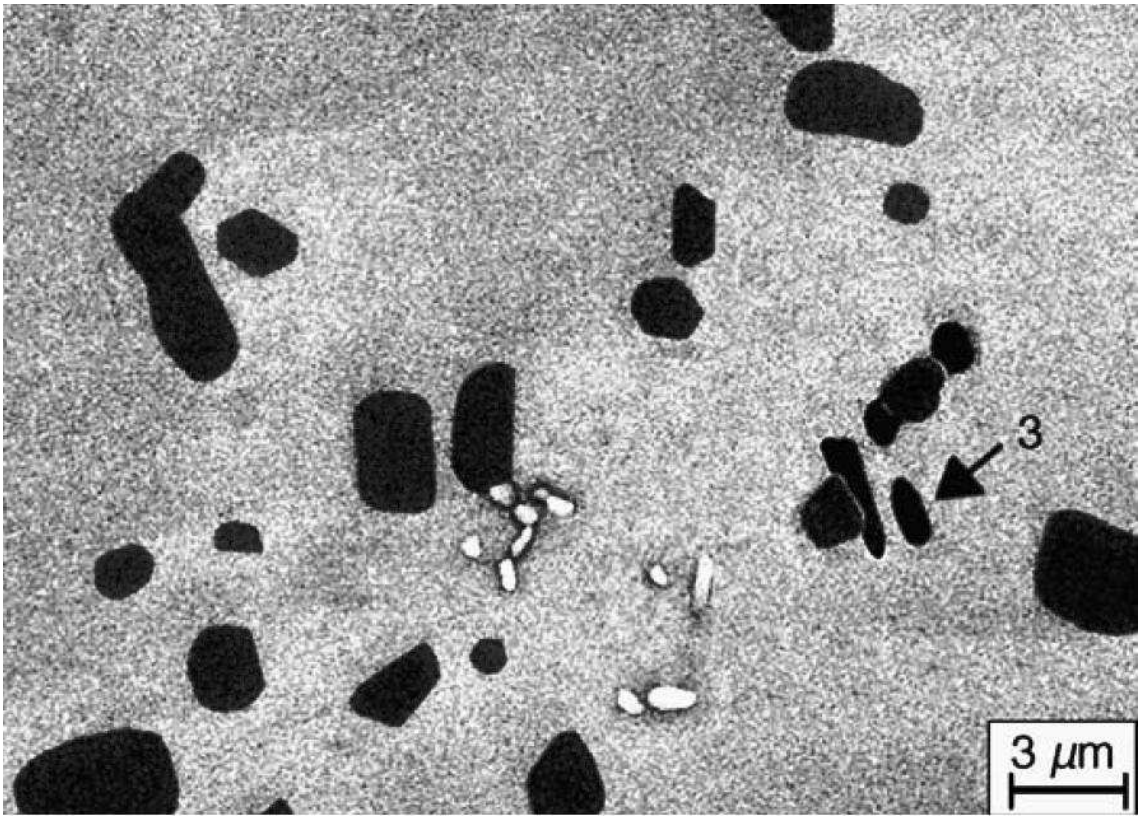

Figure 2.12: SEM micrograph showing the presence of nodular β–Al_5FeSi (arrow 3) in a 0.04wt% Be-containing alloy A357 [34].

Exposure to beryllium is associated with two pulmonary diseases, namely acute berylliosis and a granulomatous lung disease known as chronic beryllium disease (CBD) [49]. Be-containing alloys A357, C357 and D357 (Table 2.1) are therefore gradually being phased out in many applications.

2.2.1.5. Copper

Copper is limited to a maximum of 0.2% in Al-7Si-Mg alloys (Table 2.1). The addition of Cu has been claimed to lead to a higher nucleation rate and refinement of GP zones and β″-precipitates in Al-Mg-Si alloys [50,51]. However, a study of an Al-Si-Mg alloy modified with Sr found that a Cu-content higher than 0.2% resulted in a 7-fold increase of the dispersed microporosity [52]. It was postulated that copper forms interdendritic Cu-rich phases which solidify at a lower temperature. The relationship between the porosity fraction and Cu-content is shown in Fig. 2.13 [53].

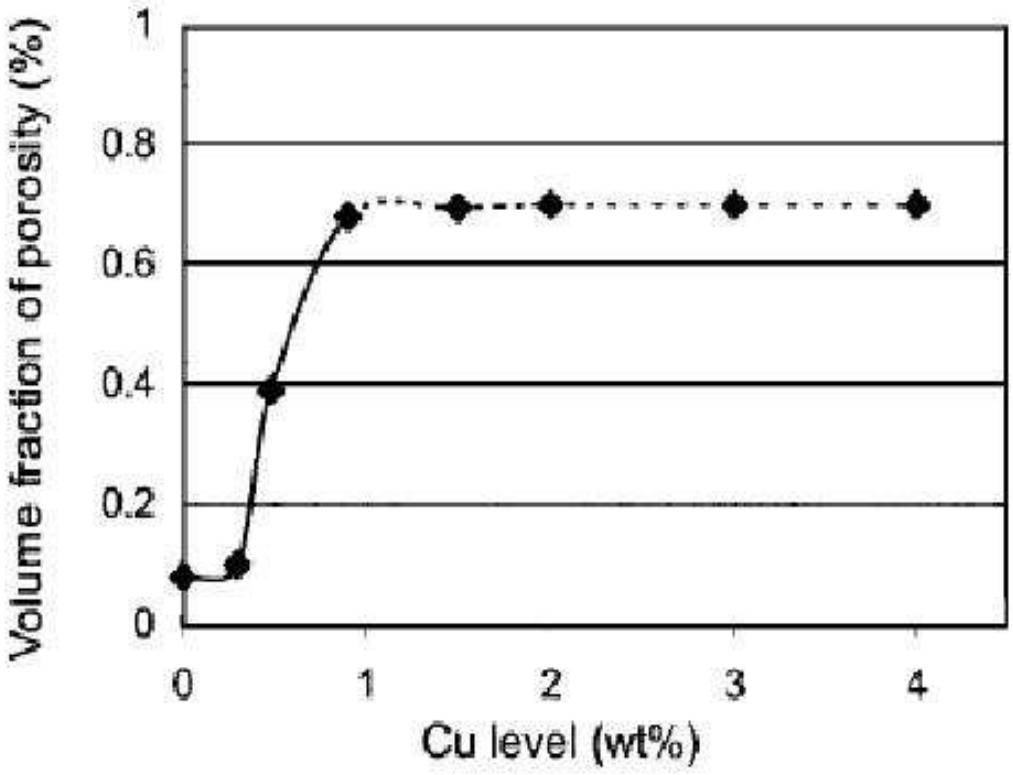

Figure 2.13: The effects of Cu content on porosity fraction in Al-Si alloy [53].

2.2.1.6. Manganese

Manganese is a common impurity in aluminium alloys and has a very limited solid solubility in aluminium in the presence of other impurities [33]. As with beryllium, manganese additions to A356/7 have been shown to modify the morphology of β-Al_5FeSi to improve the ductility of the alloy [54]. When manganese is used as a modifier, it replaces the acicular β-Al_5FeSi with a granular α-Al(Mn,Fe)Si, as shown in Figure 2.14 [54]. The combined addition of Mn and Cr has been shown to be especially effective in this regard [54]. However, the combined content of manganese, iron, chromium and other transition metals must be limited to control the formation of large fractions of coarse and brittle constituents which act as crack initiators and reduce the fracture toughness of the material [55].

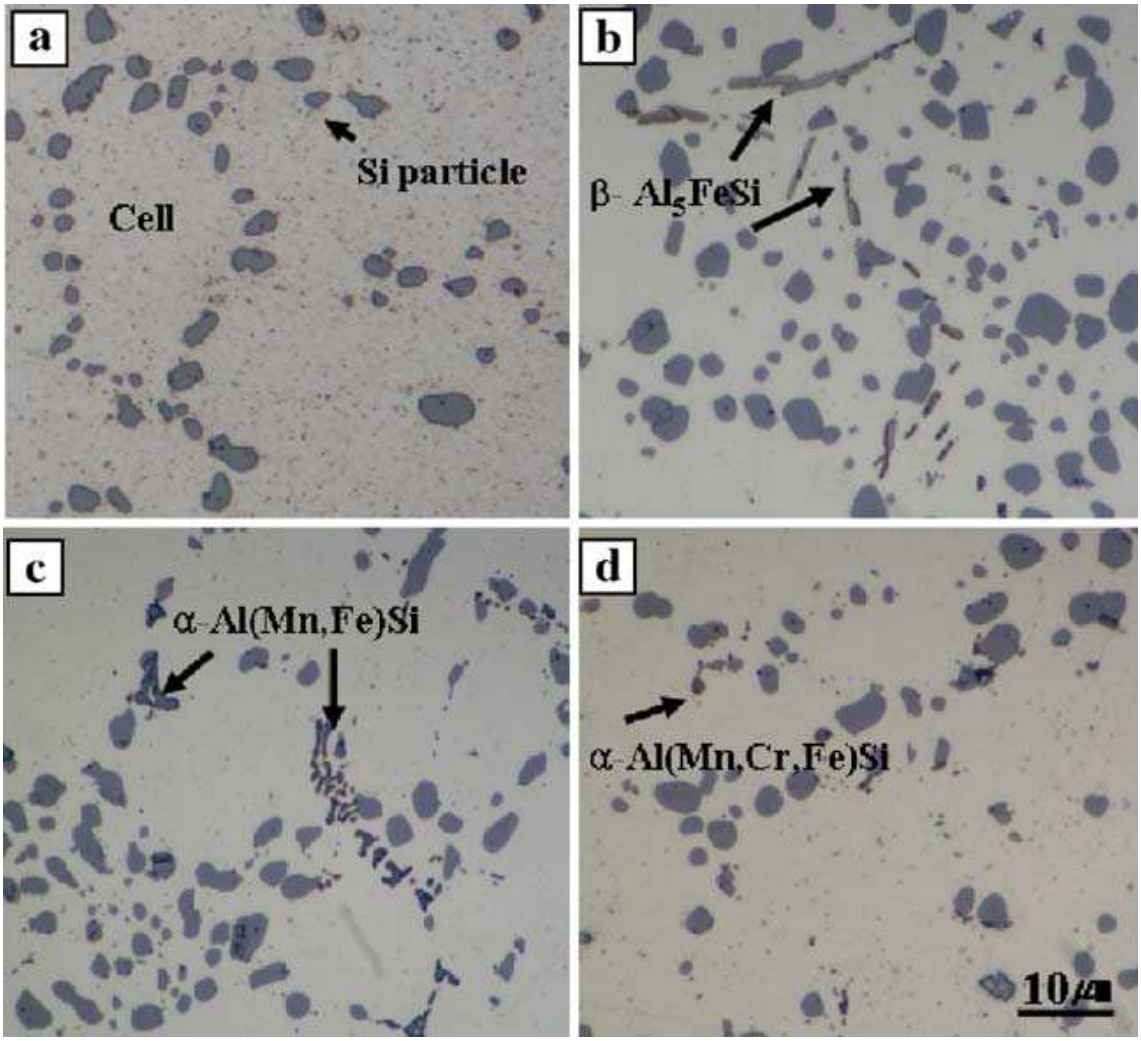

Figure 2.14: Typical solidification microstructures of (a) A356 with ~ 0% Fe, (b) A356–0.20Fe, (c) A356–0.20Fe–0.20Mn and (d) A356–0.20Fe–0.13Mn–0.13Cr [54].

2.2.1.7. Titanium

Titanium is used primarily as a grain refiner of aluminium alloy castings and ingots. When used alone, the effect of titanium decreases with time of holding in the molten state and with repeated remelting. The grain-refining effect is enhanced if boron is also present in the melt or if it is added as a master alloy containing boron combined as TiB_2 [33]. However, Figure 2.15 shows that the grain refining effect of Ti and B addition to SSM-processed alloy A356 is not very successful - an average globule circular diameter of 81μm in the A356 without Ti and B was found, with an average globule circular diameter of 78μm in the A356 with Ti and B [56].

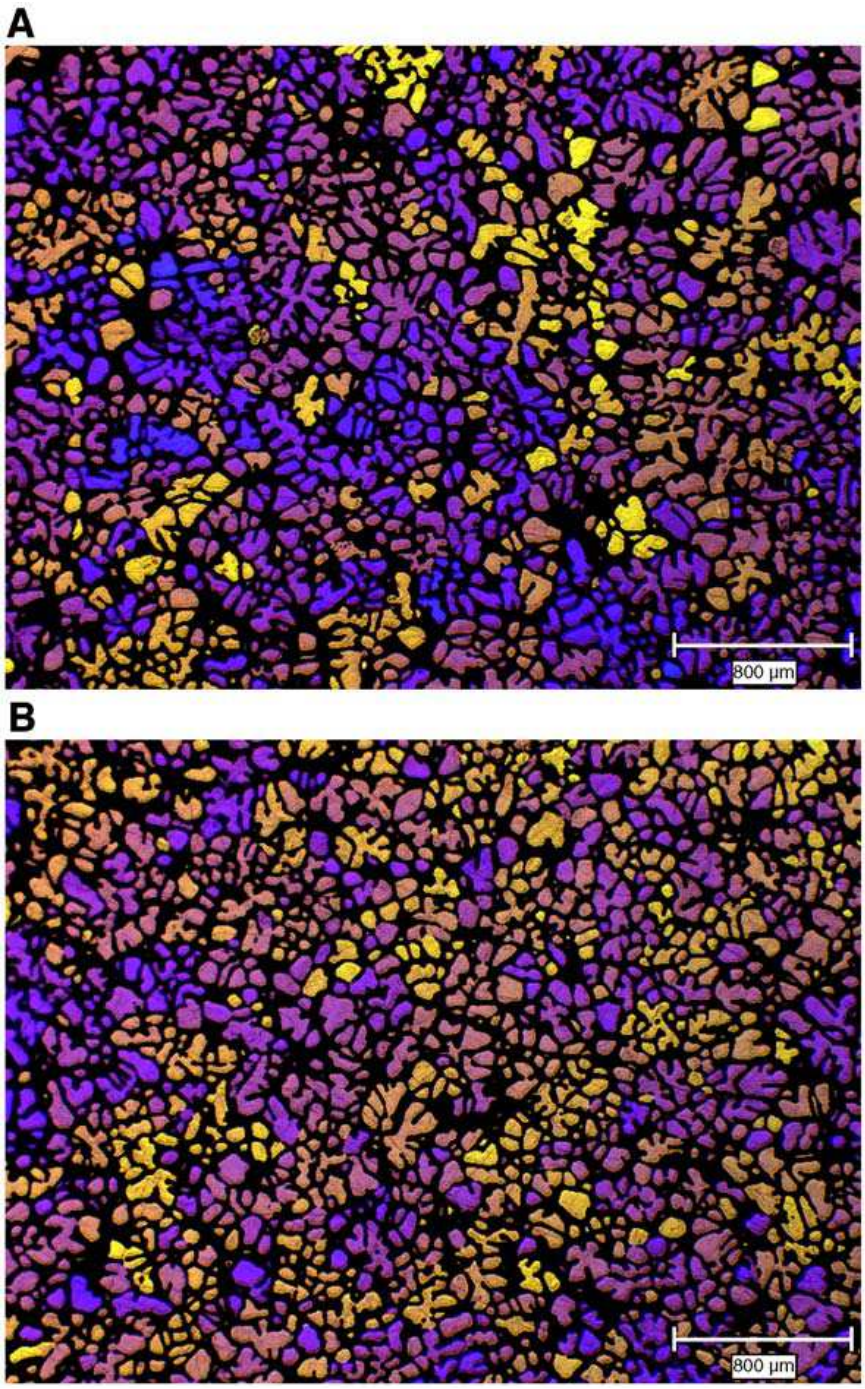

Figure 2.15: Polarised light micrographs showing the effect of Ti, B addition: (A) SSM-processed base alloy A356 without any additions; (B) SSM processed alloy A356 with the addition of 580 ppm Ti and 98 ppm B [56].

2.2.1.8. Strontium, Sodium and Antimony

The size and shape of the eutectic silicon particles can be modified with the addition of strontium, sodium or antimony [6,9]. The use of sodium as the modifying agent causes foundry problems because the fluidity of the melt is reduced. The major

difficulty is however its rapid and uncertain loss through evaporation or oxidation [9]. Additions of antimony at ~ 0.2% can also cause modification but result in a lamellar rather than a fibrous eutectic [9]. Attention has therefore been directed at an alternative method and modification is currently carried out mostly by using additions of strontium (Fig. 2.16 [57]. The amounts of strontium needed range from 0.015 to 0.02% for hypoeutectic castings, but high cooling rates during solidification reduces the amounts needed (Fig. 2.16(b)). Loss of strontium through volatilisation during melting is less than sodium and the modified microstructure can be retained if the alloys are remelted. Over-modification is not a significant problem, because excess amounts are taken into compounds such as Al_3SrSi_3, Al_2SiSr_2 and Al_4Si_2Sr [9,57]. A modification rating (MR) system classifies the eutectic Si structures commonly observed in commercial Al-Si castings by a number from one to six [58]. Table 2.2 describes the MR system in more detail [59].

Table 2.2: Modification rating (MR) system for classification of eutectic Si structures [59].

MR number	Structure	Description
1	Fully unmodified	Si is present in the form of large plates as well as in acicular form.
2	Lamellar	A finer lamellar structure, though some acicular Si may be present (but not large plates).
3	Partially modified	The lamellar structure starts to break up into smaller pieces.
4	Absence of lamellae	Complete disappearance of lamellar phase. Some acicular phase may still be present.
5	Fibrous Si eutectic (Fully modified)	The acicular phase is completely absent.
6	Very fine eutectic (Super modified)	The fibrous Si becomes so small that individual particles cannot be resolved with optical microscopy.

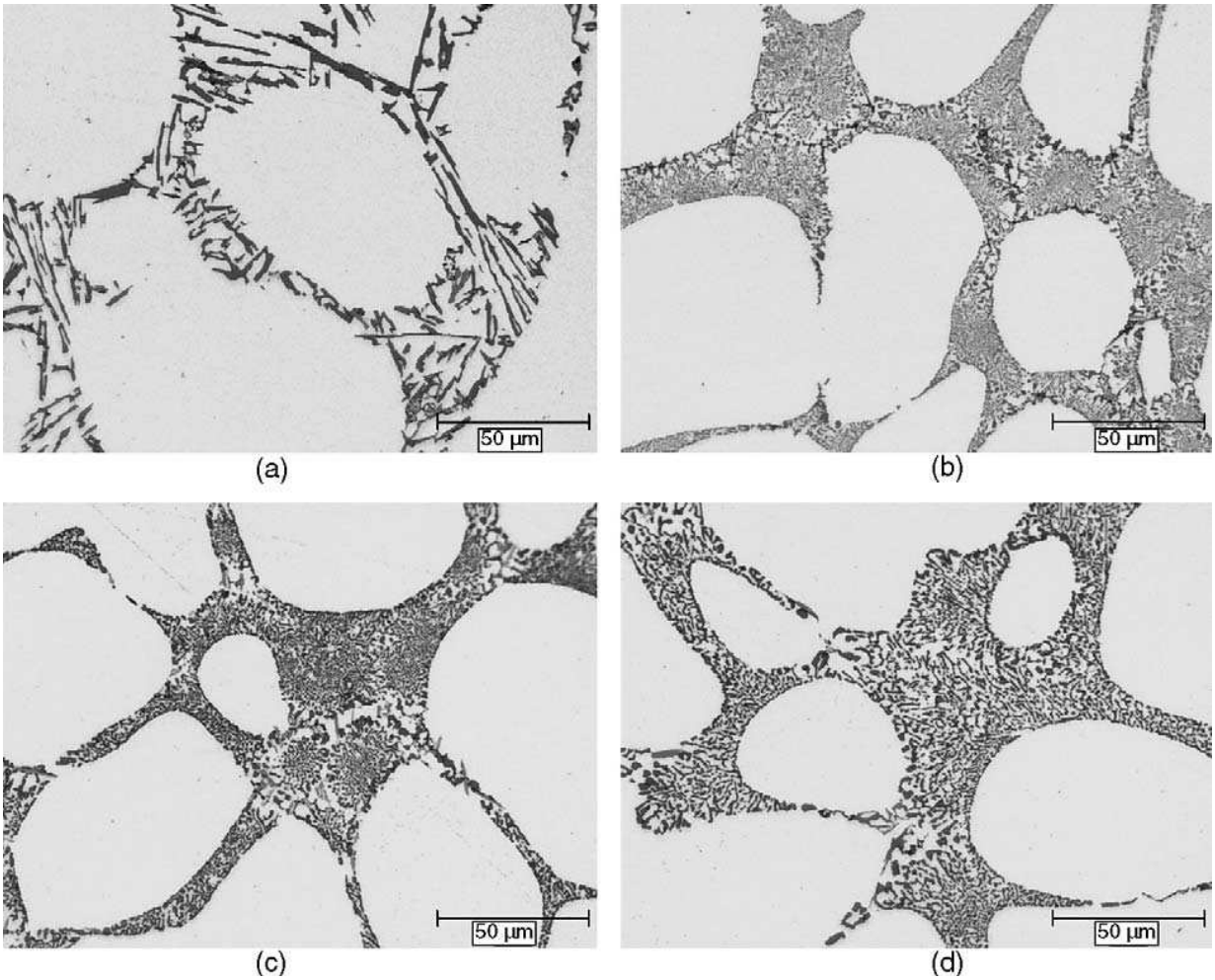

Figure 2.16: Optical micrographs showing the effect of Sr addition in SSM-processed A356 (a) non-modified with MR = 2, (b) 47 ppm Sr with MR = 5, (c) 156 ppm Sr with MR = 5, and (d) 392 ppm Sr with MR = 5 [57].

2.3. Heat Treatment

Aluminium alloys used for high-pressure die casting are mostly those based on the systems Al-Si-Mg and Al-Si-Cu, each of which has the capacity to respond to age hardening [60]. However, conventional liquid HPDC components cannot be given traditional solution heat treatments due to surface blistering and dimensional instability as a result of gas entrapment during casting [60]. Lumley and co-workers [61] have shown that liquid HPDC components can be partially solution heat treated to achieve an adequate supersaturated solid solution of the solute elements if the solution treatment stage is carried out at lower than normal temperatures (e.g. 440-490^{o}C) and for much shorter times (Fig. 2.17 [61]).

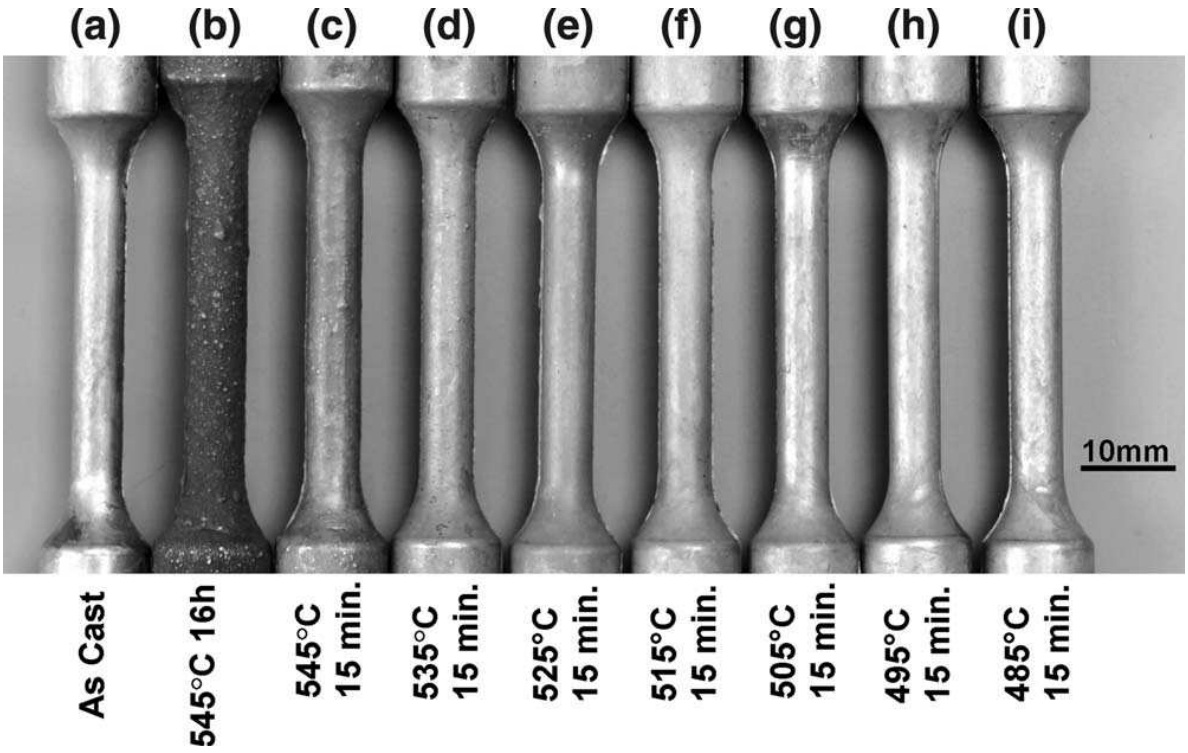

Figure 2.17: Surface appearances of Al alloy 360 in the conventionally cast HPDC as-cast condition and after different solution-treatment schedules [61].

However, one of the advantages of SSM-processing is that the laminar flow during die-fill avoids the problems of oxide and gas entrapment and also reduces the shrinkage problems during solidification [28]. Blistering during heat treatment of SSM-HPDC components can, therefore, be prevented and traditional solution heat treatments can be performed to achieve complete supersaturated solid solutions.

Heat treatment is a critical process to improve mechanical properties of certain alloy components. Heat treatment technology is currently facing numerous challenges such as energy conservation, environmental impact and the more strict market needs such as reliability, higher performance and production costs [6,62]. Additionally, heat treatment standards presently being used in foundries were developed several years ago and have to be amended to suit current foundry practices [63]. Controlled heat treatment of aluminium alloys can significantly influence properties such as strength, ductility, fracture toughness, thermal stability, residual stresses, dimensional stability, and resistance to corrosion and stress corrosion cracking [6]. The main heat treatment procedures are homogenisation, annealing, and precipitation hardening involving solution heat treatment, quenching and aging [64]. A heat treatment and temper

designation system has been developed by the Aluminium Association to describe the processing of wrought and cast aluminium alloys (Table 2.3 [6,64]).

Table 2.3: Heat treatment and temper designation system for aluminium alloys [6,64].

Suffix		Treatment
F		As-fabricated
O		Annealed
H		Strain hardened by cold work
T		Heat treated to a stable condition, excluding annealing (O)
	T1	Cooled from an elevated temperature forming process (partial solution) followed by natural aging
	T2	Cooled from an elevated temperature forming process, cold worked and naturally aged
	T3	Solution heat treated, quenched, cold worked and naturally aged
	T4	Solution heat treated, quenched and naturally aged
	T5	Rapidly cooled from elevated forming temperature and then artificially aged
	T6	Solution heat treated, quenched and then artificially aged
	T7	Solution heat treated, quenched and overaged
	T8	Solution heat treated, quenched, cold worked and then artificially aged (amount of cold work in % indicated by subsequent digit)
	T9	Solution heat treated, quenched, artificially aged and then cold worked
	T10	Cooled from an elevated temperature forming process, cold worked and then artificially aged
W		Unstable temper applied for alloys which age spontaneously at room temperature after solution heat treatment. Only specific if followed by the time of natural aging

2.3.1. Solution heat treatment

A solution heat treatment is carried out at a sufficiently high temperature for sufficiently long times to produce a nearly homogeneous solid solution [6]. The temperature is determined based on the maximum solid solubility and composition and is usually attained by heat treating near, but below, the eutectic temperature. Temperature variations within ± 6°C are allowed in most cases, but may be even stricter for some high-strength aluminium alloys [6]. Underheating can result in incomplete solution and might reduce the strengthening potential of the alloy, but is sometimes necessary for instance to avoid distortion and blistering in liquid HPDC components [60,61]. Overheating can lead to incipient melting of low-melting point phases (Fig. 2.13). The extent to which Mg and Si can be present in solid solution in alloys A356/7 depends on the actual solution treatment temperature and alloy chemistry. Fig. 2.18 shows the equilibrium concentrations of Mg and Si versus temperature in Al-Si-Mg ternary alloys in which both Si and Mg_2Si phases are present [48]. Figure 2.19 shows the 7% Si vertical section (as found in alloys A356/7) of the Al-Si-Mg equilibrium phase diagram [48]. This shows that the maximum solubility of Mg in this ternary alloy system is 0.68% at 555^{o}C. This corresponds closely to the maximum specification for alloy F357 of 0.70% in Table 2.1. Ohnishi and co-workers [65] illustrated an increase in the extent of solutionizing (with a corresponding higher strengthening potential of alloy A356) with an increase of solution treatment temperature from 500 to 570^{o}C. However, the most popular solution treatment temperature employed for Al-7Si-Mg alloys is 540^{o}C, which is 15^{o}C below the eutectic temperature [48]. From Fig. 2.18 it can be seen that the maximum solute content of Mg and Si at 540^{o}C should be 0.62 and 0.90% respectively. Using Fig. 2.19, it is seen that a 540^{o}C solution treatment temperature would result in a maximum Mg solute content of approximately 0.6% (dashed line).

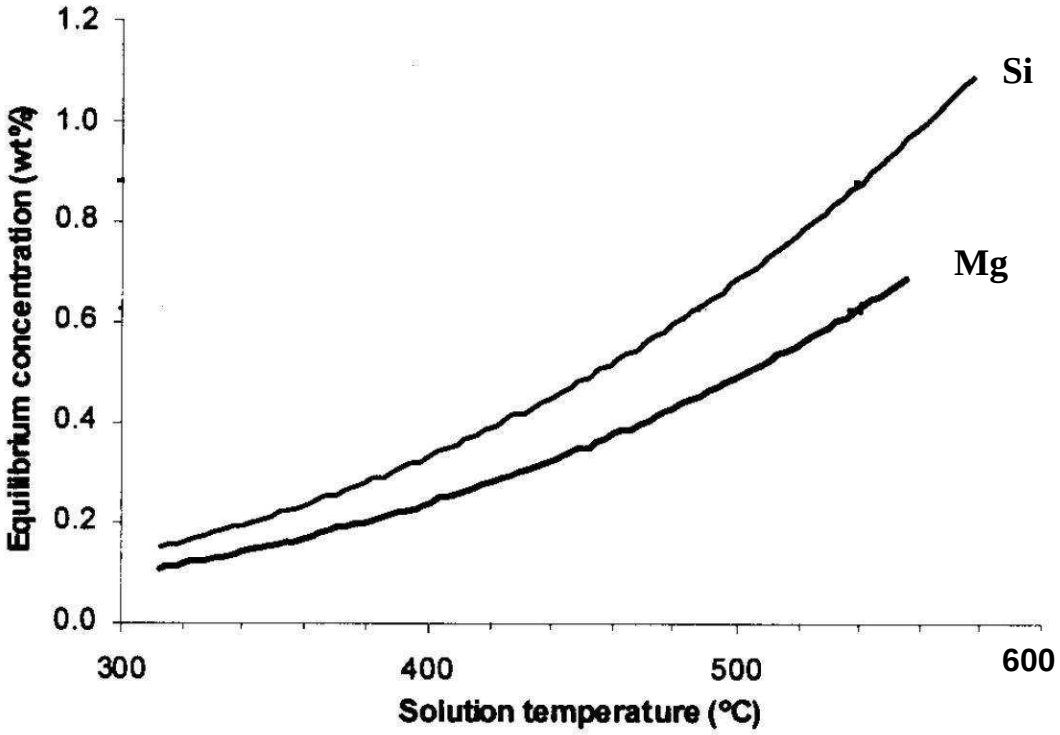

Figure 2.18: Equilibrium solute concentrations of Mg and Si in Al-Si-Mg ternary alloy system at various temperatures [48].

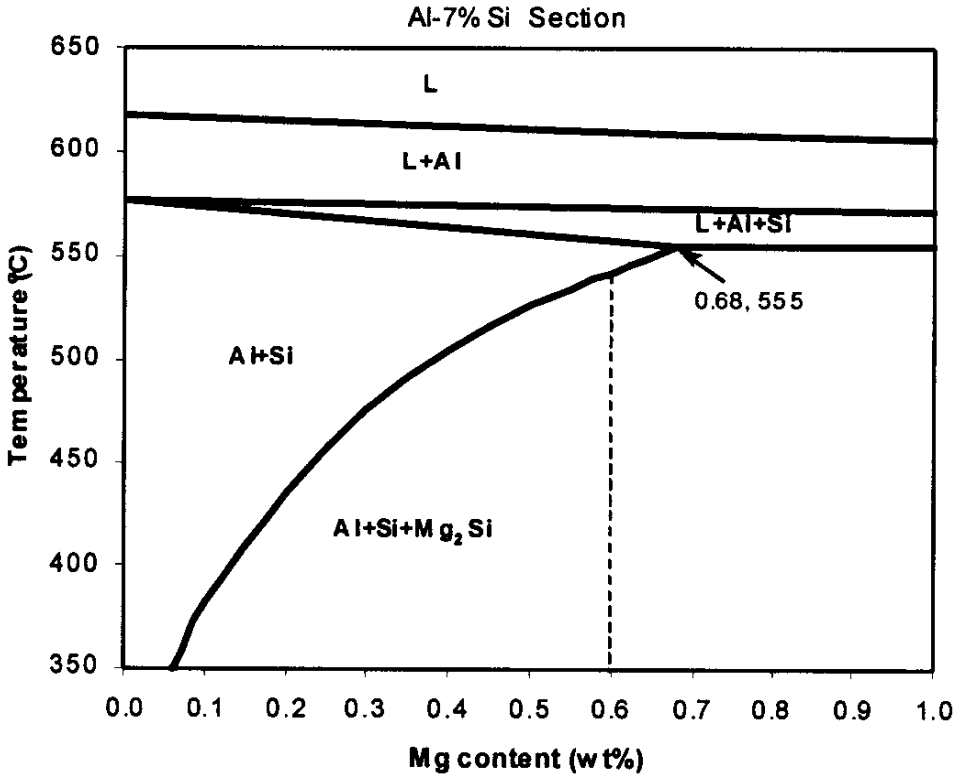

Figure 2.19: Vertical section of the Al-Si-Mg equilibrium phase diagram at 7% Si [48].

Commercial Al-7Si-Mg alloys are not pure ternary alloys and contain various impurities of which the typical ~ 0.1% Fe influences the solution treatment response the most [47,48]. Taylor and co-workers [47,48] showed that solution treatment caused a considerable transformation of the Mg-containing π-$Al_8FeMg_3Si_6$ phase to the Mg-free β-Al_5FeSi phase in alloy A356, but that this transformation did not occur in alloy F357. They found that full dissolution of the bulk Mg-content of the alloy in the matrix was possible up to 0.4%. Above 0.4% Mg, the stability of the π-$Al_8FeMg_3Si_6$ phase resulted in only partial dissolution of the bulk Mg-content of the alloy (Fig. 2.20 [48]). It can be seen from Fig. 2.20 that an F357 alloy containing 0.70% Mg and 0.12% Fe will only have 0.52% Mg in solid solution after solution heat treatment at 540°C.

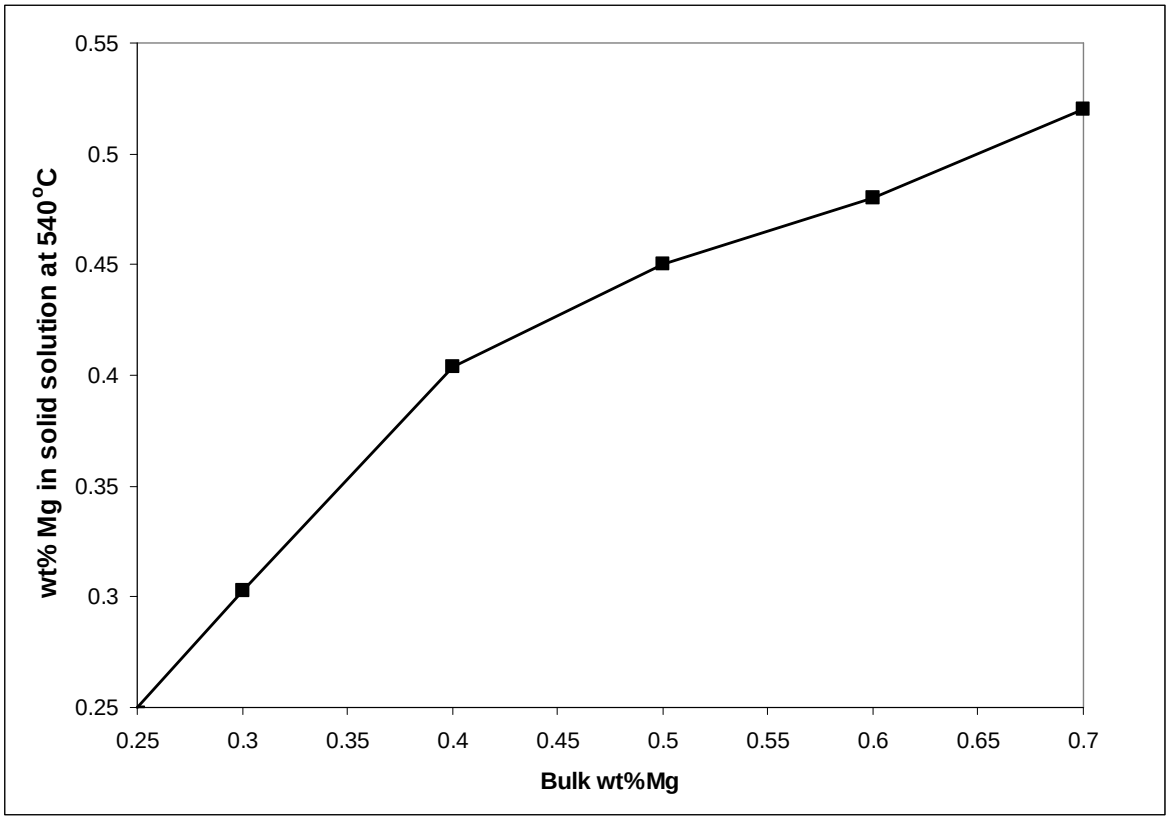

Figure 2.20: Mg-concentration in solid solution (after solution treatment at 540°C) as a function of bulk Mg-concentration in Al-7Si-Mg alloys [48].

The solution treatment time depends on the casting method, the extent of modification and the desired level of spheroidisation and coarsening of the silicon particles. Table 2.4 illustrates the differences in solution heat treatment parameters for liquid cast A356 as a function of the casting method [33].

Table 2.4: Solution heat treatment parameters for Sr-modified A356 [33].

Casting Method	Microstructural Features	Solution treatment
Sand	Large dendrite arm spacing (DAS) and globular Si particles	540^{o}C for 12 h
Permanent Mould	Fine DAS and small globular Si particles	540^{o}C for 4-12 h

Shivkumar et al [66] showed that, for permanent mould cast test bars of alloy A356, a solution treatment of only 50 minutes at 540^{o}C was sufficient to produce more than 90% of the maximum yield strength, more than 95% of the ultimate tensile strength (UTS) and nearly 90% of the maximum elongation for a given aging condition. They also demonstrated that the magnesium and silicon contents in the α-Al dendrites reached the maximum equilibrium level according to the alloy composition and that the distribution of silicon and magnesium became homogeneous within 50 minutes at 540^{o}C. Zhang et al [67] studied the possibility of using even shorter solution treatment times with A356 cast by low pressure die casting. Compared with a "traditional" 6 h solution treatment at 540^{o}C, a solution treatment of 30 minutes was sufficient to achieve more than 90% of the maximum yield strength, more than 95% of the maximum UTS and the maximum % elongation. However, only 80% of the maximum impact energy was achieved, which was attributed to a smaller silicon interparticle spacing. According to Taylor et al [48], the Mg_2Si dissolves within 5 minutes for alloy A356 and about 40 minutes for A357 during solution treatment at 540^{o}C. Homogenisation of the concentration profiles also occur rapidly – approximately 8-15 minutes for A356 and about 40-50 minutes for A357 [49]. Rometsch et al [68] performed mathematical modelling of the dissolution of Mg_2Si and homogenisation in Al-7Si-Mg alloys. The model predicts that dissolution and homogenisation are complete after solution treatment times of less than one hour at 540^{o}C for both A356 and A357. They also suggested that, from a yield strength point of view, the main objective of the solution treatment is not to dissolve the Mg_2Si particles, but rather to diffuse Mg from the eutectic matrix into the dendritic matrix. The numerical model predictions of the time required to complete Mg_2Si dissolution and alloy homogenisation at 540^{o}C for both A356 and A357 as a function of the DAS are

shown in Fig. 2.21. It can be seen that the alloy Mg content (i.e. the increase in Mg-content from alloy A356 to A357) and DAS have significant effects on the times required for dissolution and homogenisation. However, in general, less than an hour is required in all instances in Fig. 2.21.

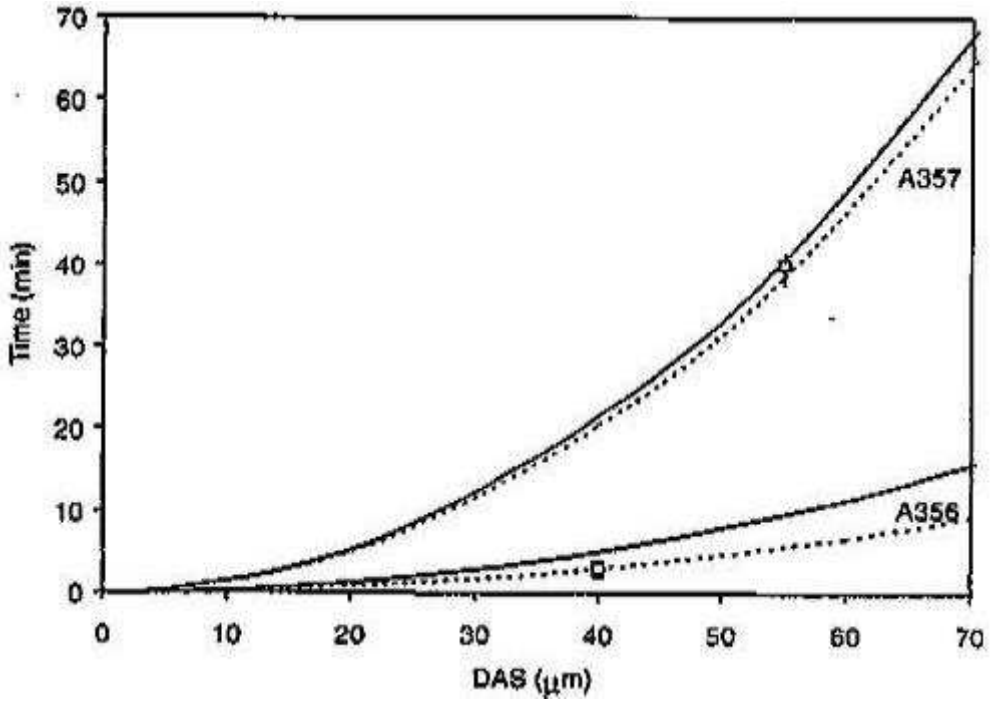

Figure 2.21: Numerical model predictions of the time required to complete Mg_2Si dissolution (dotted curves) and alloy homogenisation (solid curves) at 540°C for both A356 and A357. The vol% of Mg_2Si was kept constant in each alloy as the DAS was increased [68].

In Al-Si casting alloys, the solution treatment is also applied to cause spheroidisation of the eutectic silicon particles, which leads to improved ductility and fracture toughness (Fig. 2.22 [6]). Aluminium-silicon casting alloys, in which the eutectic silicon is modified, undergo rapid spheroidisation of the silicon particles, while complete spheroidisation is never achieved in unmodified alloys [6,69].

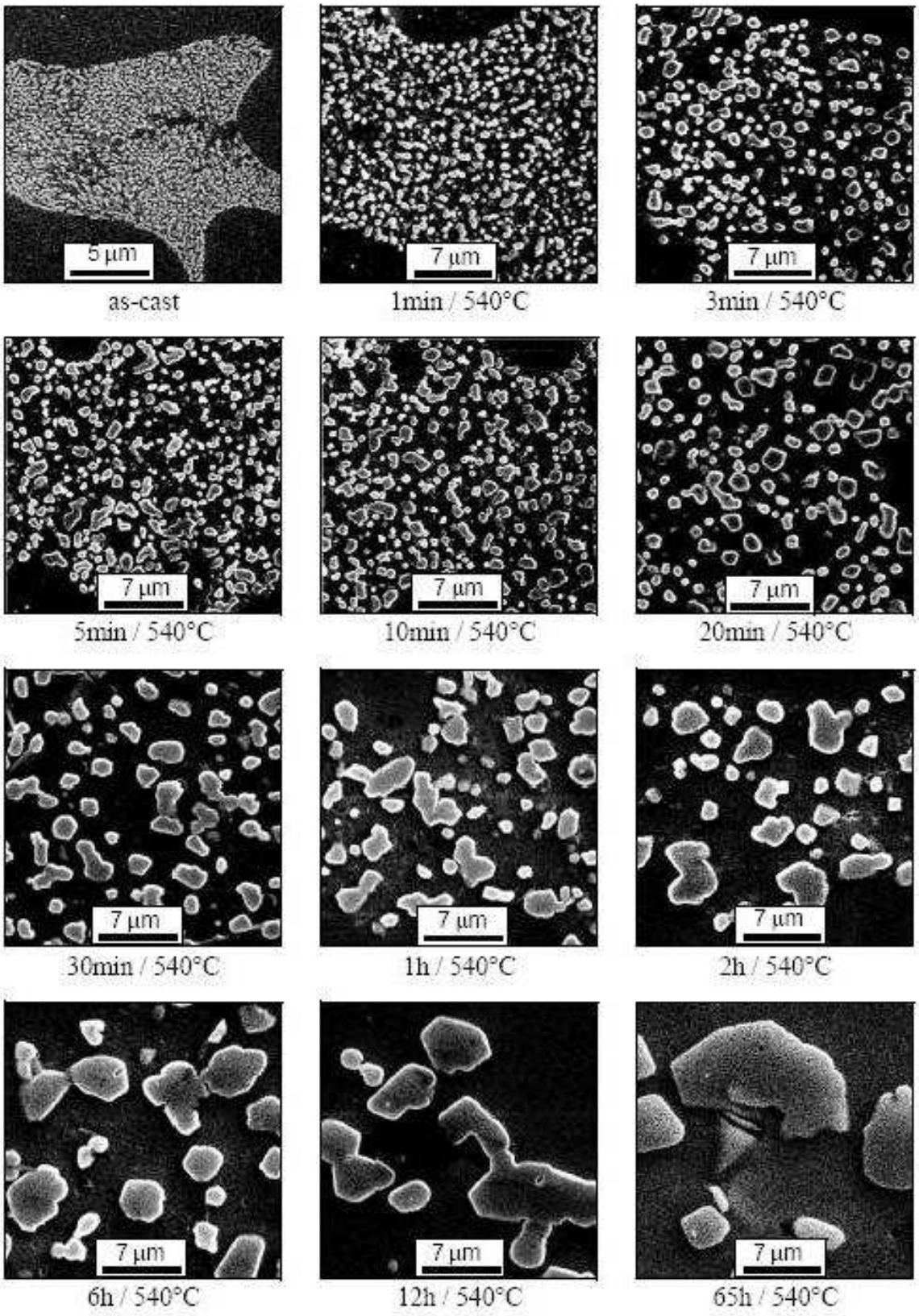

Figure 2.22: Chronology of Si spheroidisation of Sr-modified A356 at 540°C [6].

Detailed investigations on silicon spheroidisation in Sr-modified A356 by Ogris [6] have shown that the disintegration and spheroidisation of the silicon coral branches is complete within 3 minutes of soaking time between 500°C and 540°C (Fig. 2.22). This is supported by the observation by Parker and co-workers [69] that spheroidisation is complete in less than 10 minutes at 540^{o}C.

It should be noted that, apart from chemical modification by additions of Sr, Na or Sb, modification of eutectic Si-particles can also be achieved by high cooling rates during solidification [57,59,70]. It is well known that the solidification rate during HPDC is high [71] and lower levels of Sr are expected to be required to achieve modification during SSM-HPDC of Al-7Si-Mg alloys (also see Fig. 2.16).

From the above discussion, it appears as if the frequently specified solution treatment time of $\geq$ 6 h at 540^{o}C is very conservative in terms of the times actually required to achieve solute dissolution and Si-spheroidisation.

2.3.2. Quenching

Subsequent to solution heat treatment, the alloy must be cooled at a sufficiently high rate to retain the solute in solid solution and to retain a high number of vacancies at room temperature. High cooling rates associated with water quenching result in the generation of thermal stresses leading to distortion and residual stresses, especially in large castings with complex geometries [72]. Conversely, low cooling rates that provide reduced levels of thermal stress, produce non-strengthening quench precipitates (such as β′ and β in the Al-Mg-Si system), which ultimately reduce the strength attainable after aging. An optimum balance between strength and thermal stresses during quenching is therefore desired. Slower quenching rates can be achieved by using water at 65-80°C, boiling water, polyalkylene glycol, forced air or mist [72]. The average quench rates corresponding to different quench conditions, as found by Zhang and Zheng [73], are listed in Table 2.5.

Table 2.5: The average quench rates in the temperature range of 450°C to 200°C corresponding to different quenching conditions [73].

Quenching condition	25°C Water	60°C Water	95°C Water	Air Cool
Quench rate (°C/s)	250	110	20	0.5

The sensitivity of alloys to quench rate and the allowable delay between solution heat treatment and quenching is determined from quench factor analysis which is based on avoiding the tip of the nose of the Continuous Cooling Transformation (CCT) diagram. The 95% iso-yield strength contours for unmodified alloy A357 and wrought alloy 6082 are presented in Figure 2.23 [74]. Alloy 6082, with almost the same β-Mg_2Si content as A357, is much less quench sensitive than A357. The relatively high quench sensitivity of cast Al-7Si-Mg alloys is mainly due to the presence of Si particles in the structure, which affects quench sensitivity in three ways: (1) Si in solid solution diffuses to these particles, (2) particles serve as heterogeneous nucleation sites for β-Mg_2Si and (3) dislocation densities in dendrites of Al-7Si alloys are expected to be high due to localised plastic strain from the mismatch of the coefficient of thermal expansion (CTE) between Si and Al. Large differences in CTE between the Al matrix and Si particles result in the generation of compressive residual stresses in the particles and tensile residual stresses in the matrix during cooling from high temperatures. Some of the CTE mismatch is accommodated by plastic relaxation in the matrix, increasing its dislocation density, which provides more nucleation sites for quench precipitates [74].

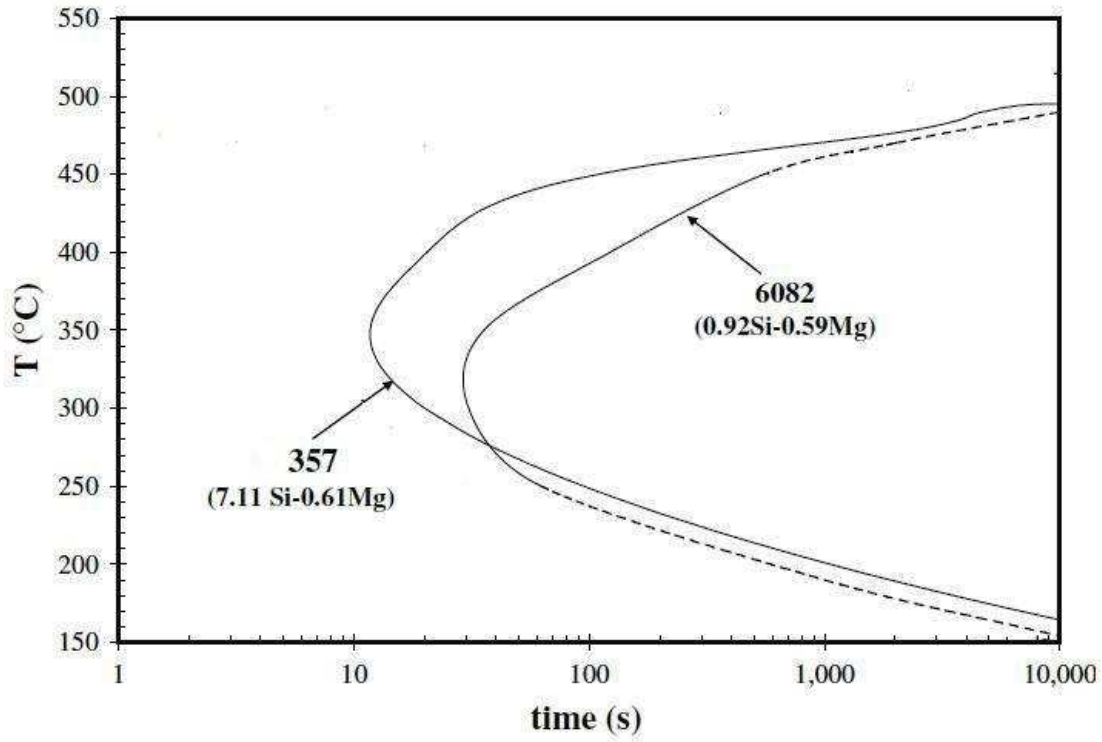

Figure 2.23: 95% iso-yield strength contours in casting alloy A357 and wrought alloy 6082 [74].

Zhang and Zheng [73] showed that the yield strength and ultimate tensile strength (UTS) of alloy A356 artificially aged at 170^{o}C for 6 h decreased significantly with decreasing quench rate (Figure 2.24). With a decrease in quench rate from 250^{o}C/s to 0.5^{o}C/s (Table 2.5), the UTS decreased from 330 to 242 MPa, i.e. by 27%, while the yield strength decreased from 274 to 184 MPa, i.e. by 33 %.

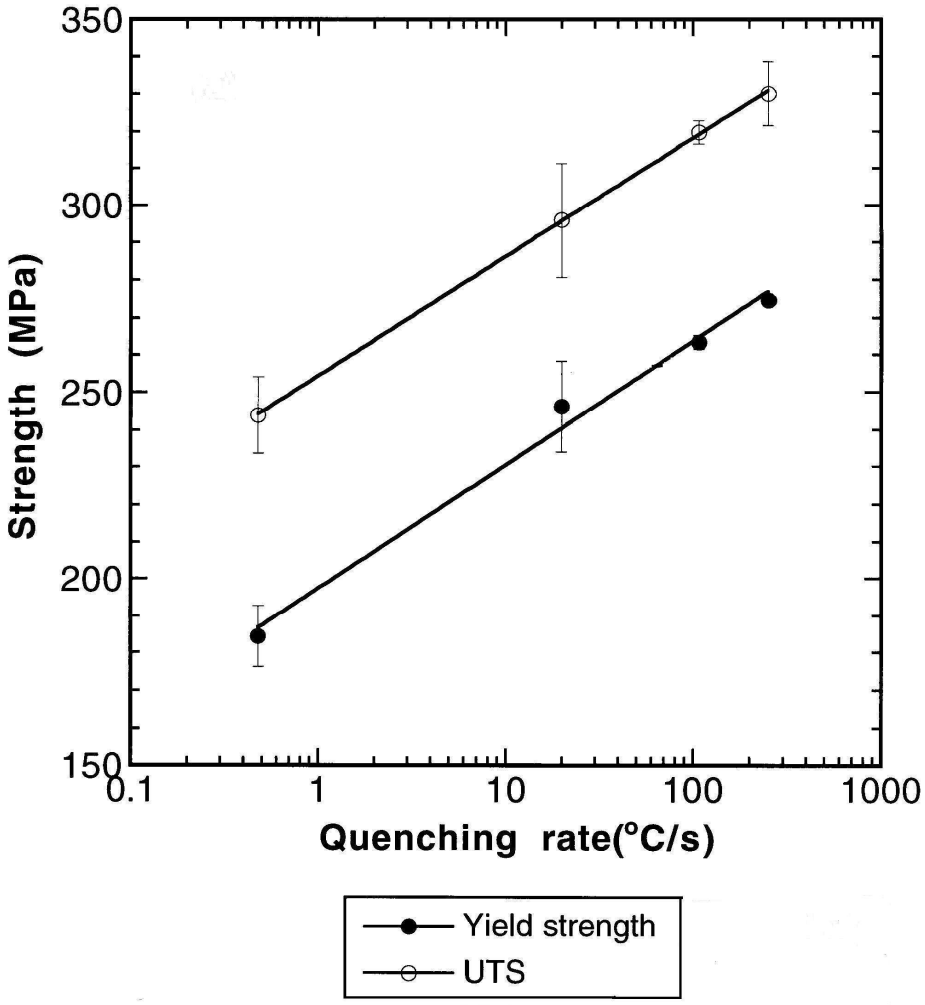

Figure 2.24: Strength of peak-aged alloy A356 as a function of the average quench rate - the quenching conditions listed in Table 2.5 were applied [73].

2.3.3. Aging

Aging is the controlled decomposition of the supersaturated solid solution to form finely dispersed precipitates in heat-treatable alloys, usually by soaking for convenient times at one or sometimes two temperature levels. Aging takes place at room temperature (natural aging) or at an elevated temperature in the range of 100–210^{o}C (artificial aging). The objective of aging is to obtain a uniform distribution of small precipitates, which gives a high strength.

The strength of an alloy is derived from the ability of precipitates to impede mobile dislocations. The strength is determined by the size and distribution of the precipitates and by the coherency of the precipitates with the matrix. The interaction with the dislocations can be described by the Friedel effect and by the Orowan mechanism [75]. Small and not too hard precipitates are normally sheared by moving dislocations

(Friedel effect – Fig. 2.25(a) [75]). When the precipitates are larger and harder, the moving dislocations bypass the precipitates by bowing (Orowan mechanism - Fig. 2.25(b) [75]). The strength of the precipitates increases with their size as long as they are sheared by dislocations. Further increase of precipitate size makes the shearing processes more difficult; hence, it is more favourable for the dislocations to pass the precipitates via the Orowan mechanism. This leads to a decrease in strength with further increase in precipitate size (Fig. 2.25(c) [75]). The highest strength is obtained when there is an equal probability for the dislocations to pass the precipitates by shearing and by bowing [75]. Figure 2.25 is used in the process model for age hardening of Al-7Si-Mg alloys (see Chapter 6).

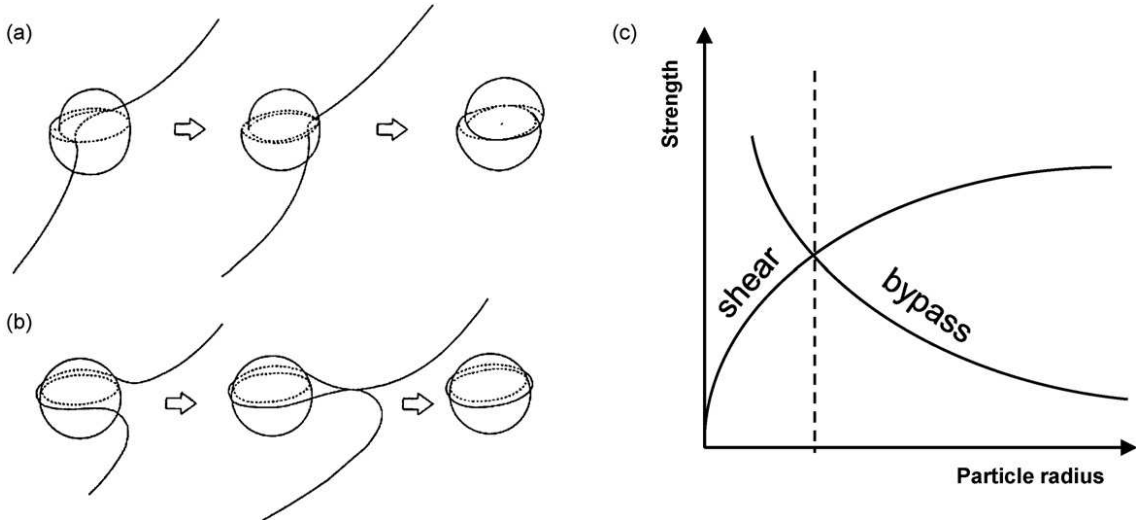

Figure 2.25 [75]: Dislocations pass precipitates either by (a) shearing or (b) bypassing [76]. (c) Relationship between precipitate radius and strength of the particles to resist shearing or bypassing by dislocations [9].

It is often assumed that the precipitation sequence (equation 2.1) and phases in the Al-Mg-Si 300 series casting alloys are similar to those in Al-Mg-Si 6000 series wrought alloys [11]. To date, there is a lack of detailed research work revealing precipitate micro- and nanostructural evolution during aging of the Al-Si-Mg casting alloys. This is due to difficulties the eutectic component causes in preparing high-quality samples for transmission electron microscopy (TEM) and atom probe tomography (APT) [11]. The nanostructural evolution of the Al-Mg-Si 6000 series wrought alloys has been studied much more extensively than the casting alloys [77-79]. The main difference between the 300 series and 6000 series is the Si content, with the casting alloys

containing a significantly higher quantity of this alloying element (Table 2.1). The 6000 series wrought alloys generally contain ≤ 1.5% Si and ≤ 1.2% Mg respectively [80]. The following discussion on the aging characteristics of Al-Si-Mg alloys will therefore also incorporate studies on the precipitation of the 6000 series wrought alloys.

2.3.3.1. Natural aging

Natural aging refers to the decomposition of the solid solution that occurs at room temperature. During natural aging, the high level of supersaturation and the high vacancy concentration from rapid quenching cause quick formation of clusters and hardness and strength increases swiftly (Fig. 2.26) [80]). The change in hardening rate in Fig. 2.26 from fast to slow was attributed to a decrease in the growth rate of the clusters. Initially, silicon dominates cluster formation due to its higher diffusivity and lower solubility in aluminium. Later (i.e. after approximately 50 minutes), the clusters begin to enrich in Mg and hardening occurs at a lower rate due to cluster growth that is limited by Mg diffusion [80].

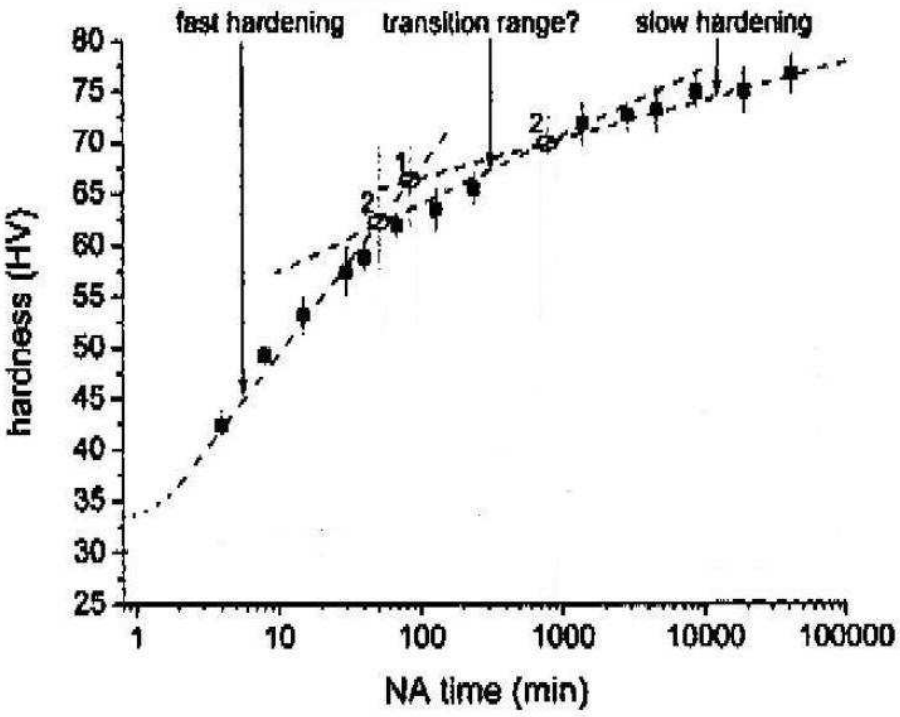

Figure 2.26: Hardness evolution of Al-0.59% Mg-0.82% Si naturally aged at 25°C after solution heat treatment and quench [80].

Nearly maximum stable values are attained in 4 or 5 days for Al-7Si-Mg alloys and the T4 temper is therefore usually specified as material that was naturally aged for 120 hours [81]. The solute clusters that are found in large numbers in Al-Mg-Si alloys in the T4 condition typically contain only a few to tens of solute atoms [78]. They are fully coherent with the matrix and are difficult to resolve even by employing HRTEM (Fig. 2.7(a)) and a technique such as APT is required for their study (Figure 2.27 [78]).

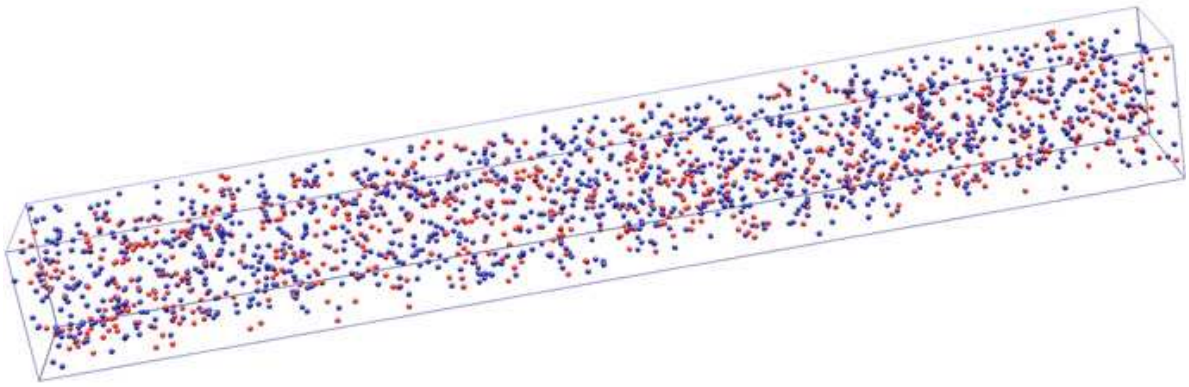

Figure 2.27: 3-dimensional reconstruction of Mg (red spheres) and Si (blue spheres) atom positions in a Al–0.59% Mg–0.82% Si alloy after solution heat treatment with subsequent aging at room temperature (NA) for 1 week. The investigated volume is 8.5x8.5x62 nm^3 [78]

It was postulated that only about 5% of all Si and Mg atoms in the naturally aged specimen in Fig. 2.26 were located in the clusters and that such clusters consisted of only about 4–8 atoms [78].

2.3.3.2. Artificial aging

Artificial aging involves decomposition of the supersaturated solid solution at elevated temperature, normally in the range of 100-210°C for times between 2 h to 48 h [6]. At these temperatures, atoms can move over larger distances and the precipitates formed during artificial aging are normally much larger in size than clusters and GP zones [75]. The artificial aging treatment is designed to produce optimum size, distribution, constitution and morphology of precipitates.

The most comprehensive sets of artificial aging curves for Al-7Si-Mg alloys A356/7 have been determined by Rometsch and Schaffer (Figures 2.28 and 2.29 [82]). These

curves were produced after a solution treatment at 540°C for 75 minutes (A356) and 120 minutes (A357), quenching in room temperature water and artificial aging without delay (i.e. no natural pre-aging).

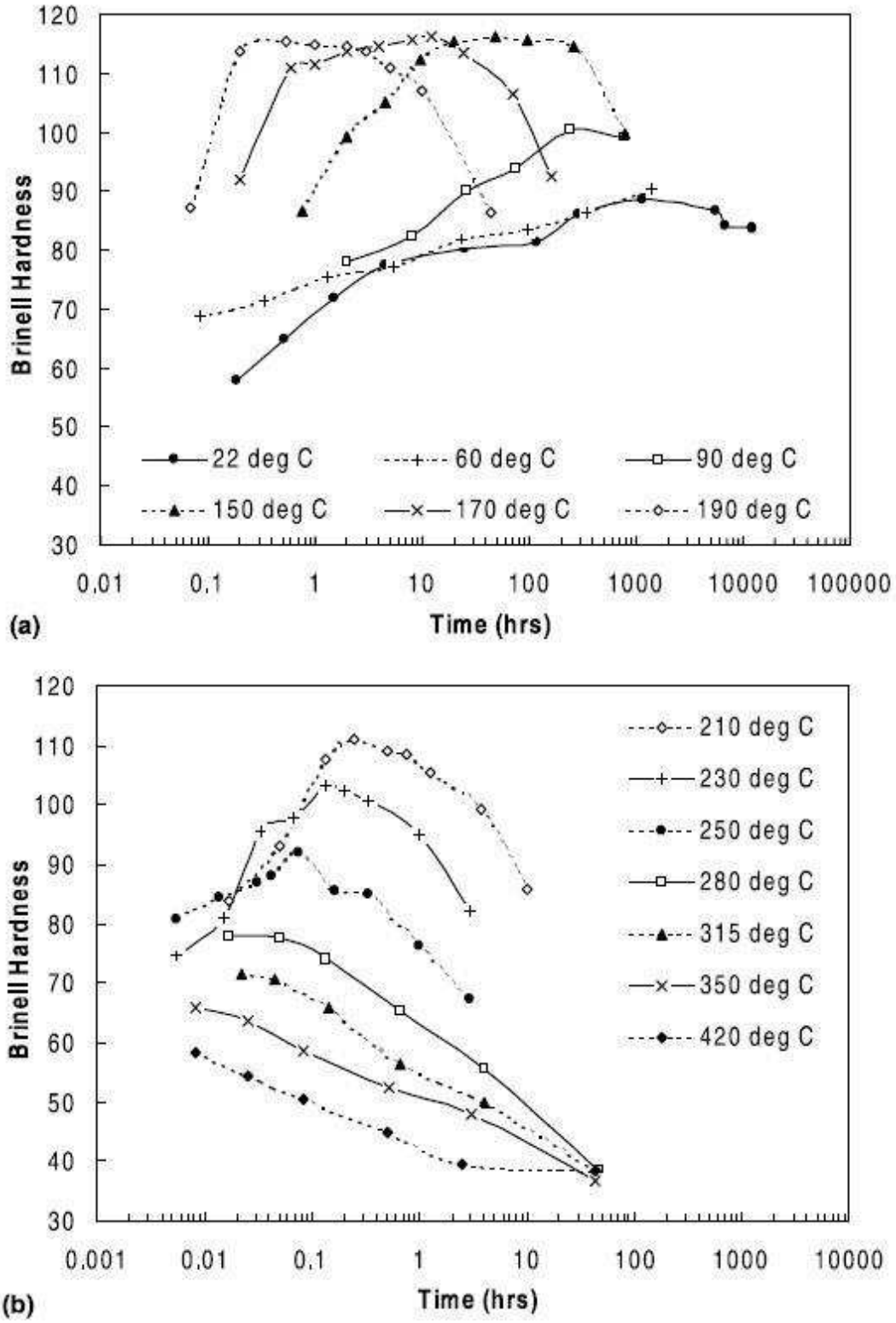

Figure 2.28: HB aging curves for A356 at (a) 22–190°C and (b) 210–420°C [82].

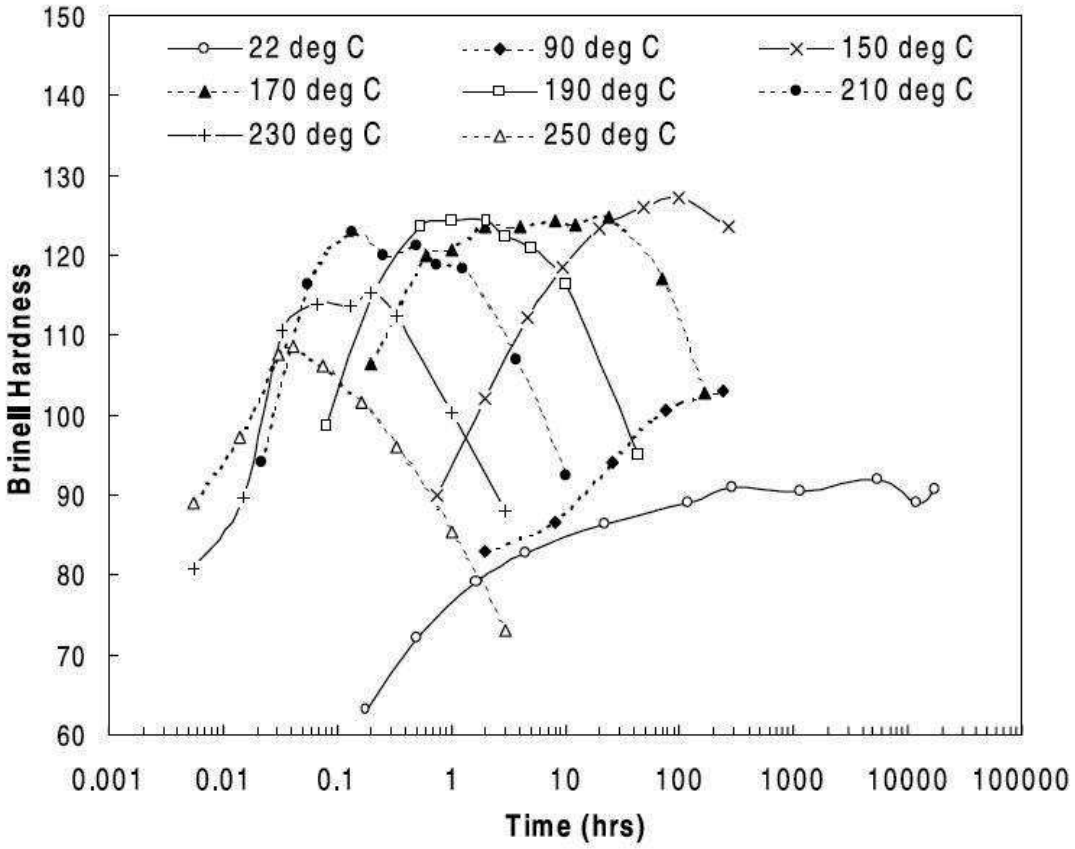

Figure 2.29: HB aging curves for A357 at 22–250°C [82].

When artificial aging temperatures in the range of 170–210°C are used, comparable strength levels are achieved in Figs. 2.28 and 2.29. The time for aging can, however, be shortened if a higher temperature is used - the time to peak hardness is about 10 h at 170°C, while it is only 20 min at 210°C. If the artificial aging temperature is increased above 210°C, a decrease in strength is seen. According to Eskin [83], the β″-phase is substituted by the β′-phase at temperatures above 200°C, which gives a lower contribution to strength.

The precipitation sequence of alloy A356 was recently studied by Rinderer et al by employing TEM and APT [11]. Sample preparation of casting alloys presents more difficulties than the wrought alloys and APT measurements of only ~ 0.5 million atoms were achieved. The success rate for measurement of the A356 alloy was also reduced compared to the 6000 wrought alloys. Castings were studied after solution heat treatment at 540°C for 6h followed by a 60°C water quench. Natural aging was for 2 h prior to artificial aging at 180°C and aging was performed at various times of

0.25 h, 1 h, 2 h, 196 h and 670 h with 2 h representing the peak hardness condition. The TEM sequence of precipitation is shown in Fig. 2.30 [11].

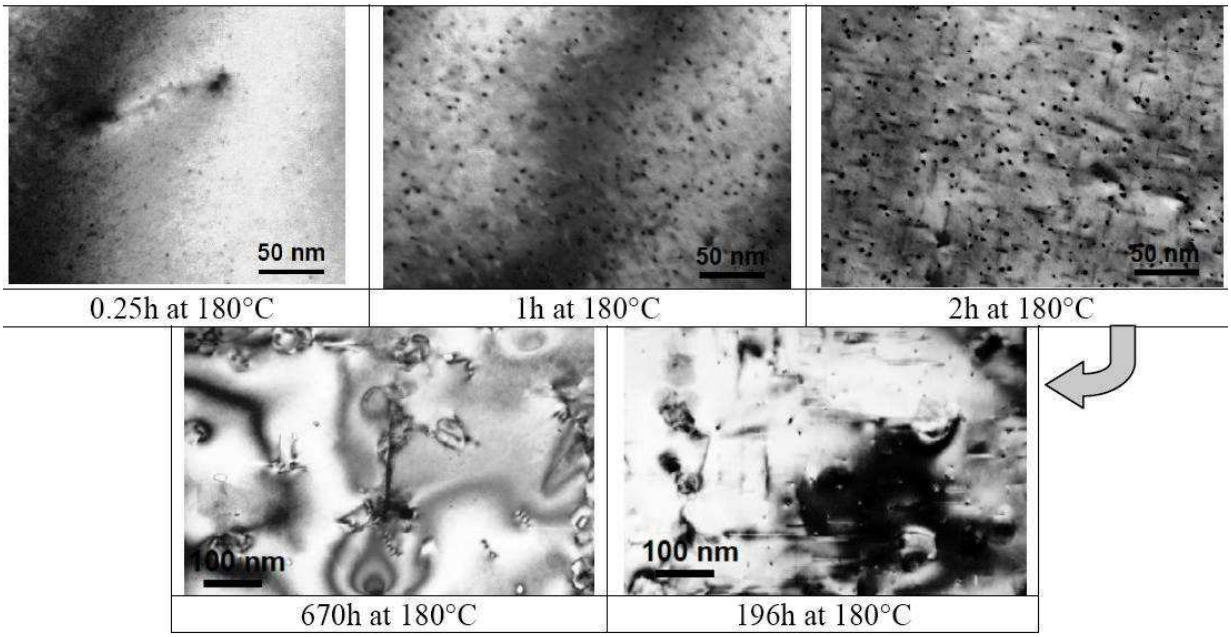

Figure 2.30: TEM bright field micrographs illustrating the precipitation sequence in A356 alloy aged at 180°C for various times [11].

After artificial aging for 0.25h at 180^{o}C, the TEM micrograph shows a microstructure that contains a uniform dispersion of fine spherical particles (i.e. GP zones) and a very small amount of fine needle-like precipitates on dislocations. After aging for 1 h the microstructure includes fine-scale $<100>_{\alpha}$ precipitate needles which are most likely the β″-phase. In the peak aging condition of 2 h, the microstructure shows a higher proportion of β″. Over-aging for 196 h results in a microstructure consisting of a mixture of coarse $<100>_{\alpha}$ rods (most likely the β′-phase). Long-term aging for 670 h at 180°C only led to a significant coarsening of β′ and precipitates of the equilibrium β-phase were not detected.

3D atom probe analysis was performed on A356 samples in the under-aged (0.25 h at 180°C) and peak aged (2 h at 180°C) conditions (Fig. 2.31 [11]).

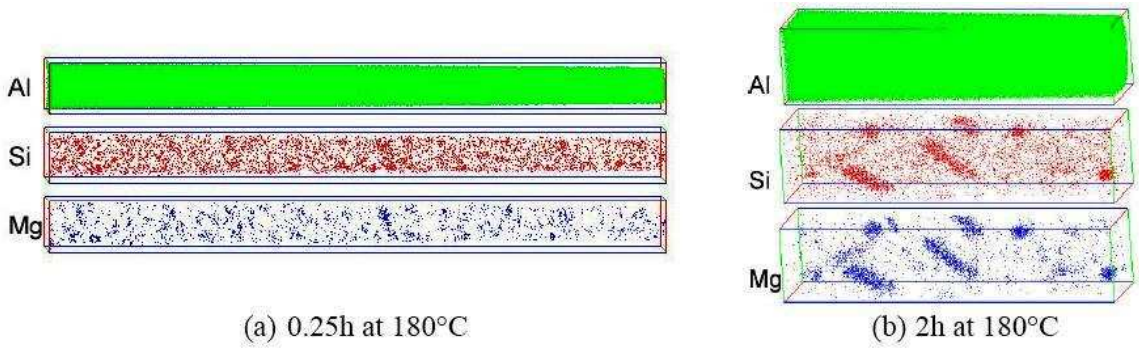

Figure 2.31: 3D-APT results for A356 alloy aged at 180°C. For the under-aged condition (a), the volume shown is 14x14x166 nm^3 and the analysis volume for the peak aged sample (b) is 20x19x88 nm^3 [11].

In the under-aged condition the number density of Mg/Si aggregates was found to be ~ 7 x 10^{23} m^{-3} and, on average, the Mg/Si ratio of the aggregates was ~ 0.7. For the peak aged condition, the composition of the precipitates had an average Mg/Si ratio of ~ 1.2, i.e. the additional aging time resulted in an increase in the Mg associated with the precipitates. The number density of particles decreased to 4 x 10^{23} m^{-3} and this reduction in the number density of particles was accompanied by coarsening of the precipitates compared to the under-aged condition [11].

2.3.3.3. Influence of natural pre-aging on subsequent artificial aging

The influence of prior natural aging time on the subsequent artificial aging response of Al-Mg-Si wrought 6000 series alloys is complex, but has been studied extensively [50,80,84-87]. In the more highly alloyed alloys within the 6000 series it has been suggested that clusters that form during natural aging are “robust” during subsequent artificial aging [9,84]. They proposedly trap the available vacancies or deplete the matrix from solute atoms, while also not being favourable nucleation sites for further in-situ heterogeneous nucleation of β″ [86]. For instance, the number density of β″ precipitates in alloy 6082 has been shown to be almost five times higher in samples that were artificially aged immediately after solution treatment compared to samples that were naturally aged for a week before artificial aging [84], which had an adverse effect on the tensile properties [9,85]. The opposite, however, is believed to occur in the 6000 series alloys that are not as highly alloyed [9,50,85]. Chang and co-workers [50] described the “positive effect” of natural pre-aging on precipitation hardening in a wrought alloy with a composition of Al-0.44at%Mg-0.38at%Si. Artificial aging of

naturally aged samples increased the value of the peak hardness which was attributed to an increase in the number density of β″ needle-like precipitates as compared to samples without prior natural aging. Bichsel and Ried [87] have drawn contour plots for 6000 series wrought alloys showing the effect of 24 h natural aging on the change in UTS (MPa) as a function of the Mg and Si content (Fig. 2.32 [85]). The contour lines indicate the change in UTS after artificial aging at 165^{o}C for 15 h. Figure 2.32 confirms that the negative effect of natural pre-aging is obtained in 6000 series alloys with high Si and Mg contents, whereas the opposite occurs in alloys with low Si and Mg contents.

Gupta et al [88] have used differential scanning calorimetry (DSC) to study precipitation in a naturally pre-aged wrought Al-Mg-Si alloy (Fig. 2.33). The curve shows two exothermic precipitation peaks B and D, and three dissolution troughs, A, C and E. Peak B is a composite peak and was attributed to precipitation of β″/β′, while peak D was attributed to precipitation of β particles. The trough A is consistent with the dissolution of some of the zones and clusters that are typically present in the T4 temper alloys.

The effects of natural pre-aging on artificial aging of 300 series casting alloys have not been studied as comprehensively as for the 6000 series wrought alloys and only mechanical testing studies have been conducted with a lack of microstructural investigations. Emadi et al [72] found that natural pre-aging of A356 was detrimental to yield strength and UTS, although the properties seemed to recover after a delay of 20 h for bars aged at 170^{o}C (Fig. 2.34 [72]. Ductility was improved up to 12 h natural aging and then dropped significantly for 20 h natural aging [Fig. 2.34 [72]). The authors concluded that the reasons for the observed behaviour are not clear. A recent review paper [75] on the heat treatment of Al-Si-Mg-(Cu) casting alloys concluded that the influence of natural pre-aging on the subsequent artificial aging is not yet fully understood and needs to be studied further.

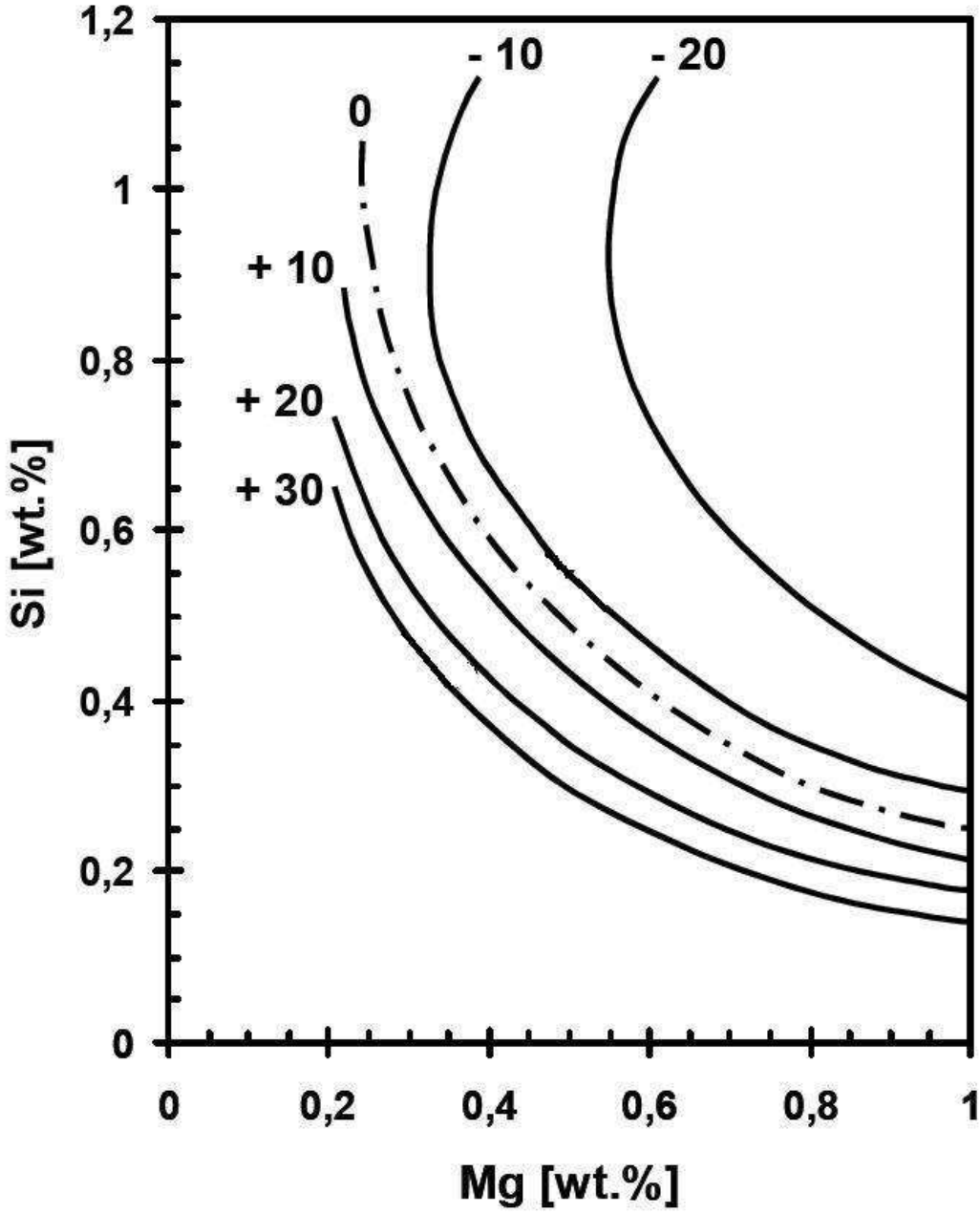

Figure 2.32: Contour plots for 6000 series alloys showing the effect of 24 h natural pre-aging on the change in UTS (MPa) after artificial aging at 165°C for 15 h as a function of the Mg and Si content [85].

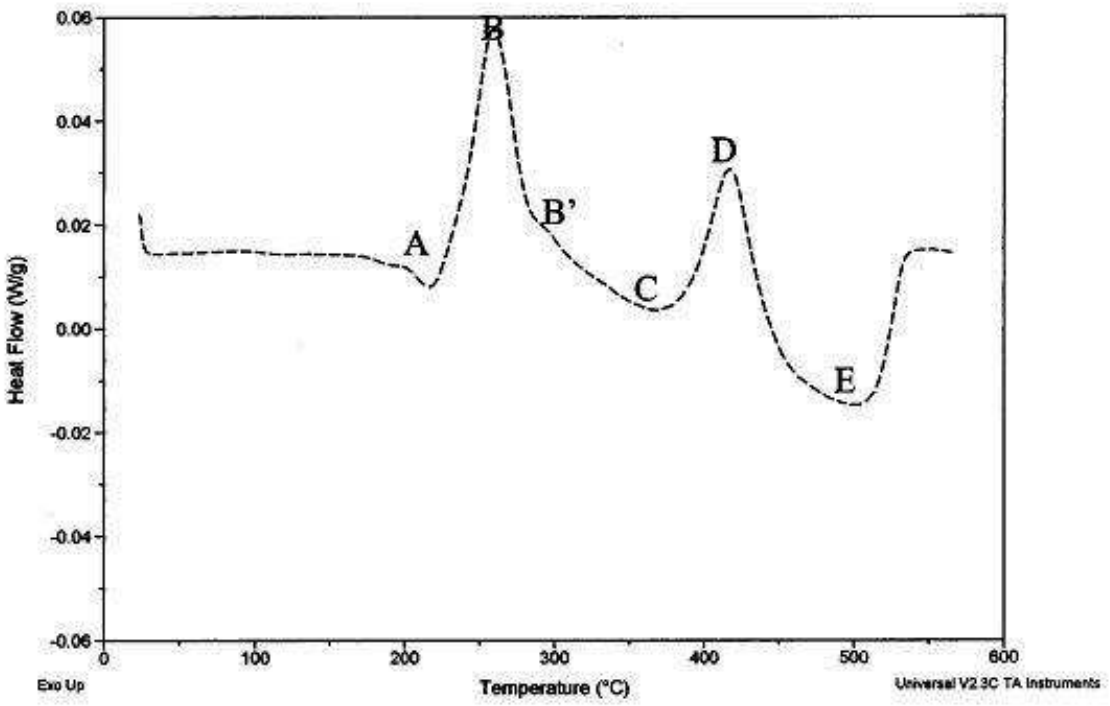

Figure 2.33: DSC curve of a wrought Al–Mg–Si alloy in the T4 condition with 1.26wt% Mg_2Si [88].

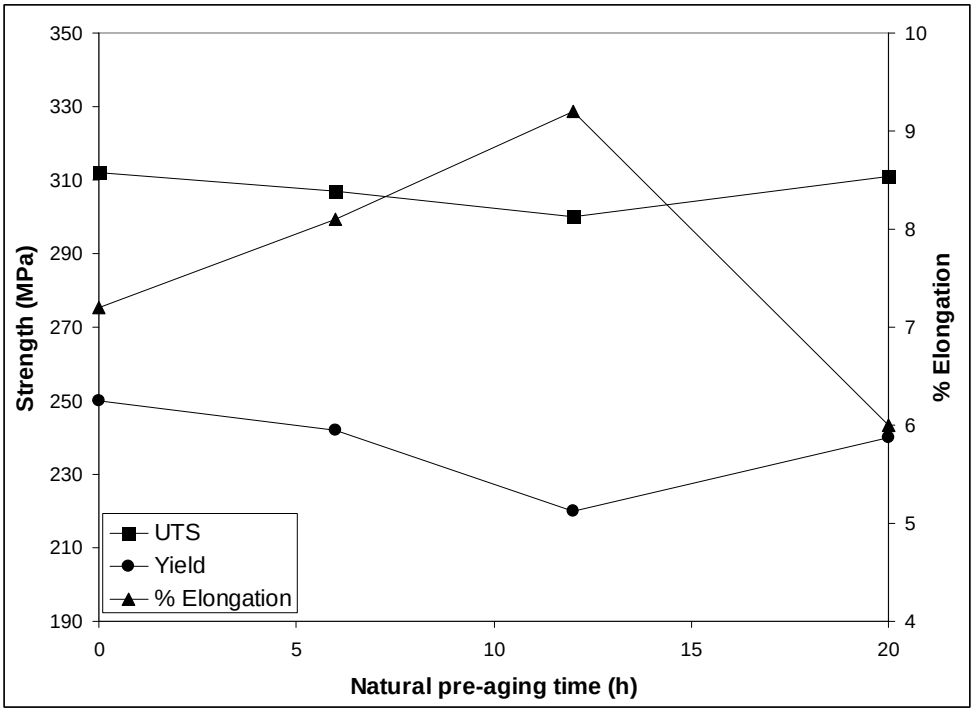

Figure 2.34: Effect of natural pre-aging time on yield strength, UTS and %elongation of A356. Heat treatment consisted of solution treatment at 540°C for 3 h, a room temperature water quench, natural pre-aging and artificial aging at 170°C for 6 h [72].

2.3.3.4. Heat treatment response of SSM-processed Al-7Si-Mg alloys in comparison with conventional liquid cast alloys

According to Dewhirst [12], after the mechanisms for SSM heat treatment were commercialised, the first heat treatments applied to it were essentially those already in use for dendritic materials. These treatment regimes are not necessarily the optimal ones as the different microstructure and solidification history of SSM components should be considered.

The American Society for Testing and Materials (ASTM) Standard B969 from 2010 named "*Standard Specification for Aluminum-Alloy Castings Produced by the Squeeze Casting, Thixocast and Rheocast Semi-Solid Casting Processes*" recommends heat treatment parameters for SSM-cast A356 and A357 as shown in Table 2.6.

Table 2.6: ASTM B969-10 recommended heat treatment parameters for semi-solid thixocast and rheocast castings.

Alloy	Final temper	Solution heat treatment		Precipitation heat treatment	
		Metal temperature ± 5°C	Time at temperature (h)	Metal temperature ± 5°C	Time at temperature (h)
A356	T5	-	-	160	6-12
	T6	540	4-10	160	3-6
A357	T5	-	-	170	6
	T6	540	10	170	6

In this standard it is recommended that the quench after solution treatment should be carried out in water at 65-100°C. Recommendations on natural pre-aging and its influence on subsequent artificial aging are not included.

Only limited work has been performed on the optimisation of the solution heat treatment of SSM processed A356/7. In the casting industry, it is often specified that a dendritic (especially permanent mould cast) A356 component should be solution

treated for 6 hours at 540^{o}C [67]. This has also been the most popular solution heat treatment used for SSM-processed A356 [81,89]. According to Dewhirst [12], the time needed for the solution treatment for semi-solid metal processed A356 should be less than for dendritic A356 due to shorter diffusion paths (due to a globular microstructure) and because the thermal history of SSM-processed components promotes enhanced solutionising before heat treatment commences. Rosso and Actis Grande [90] proposed that a solution heat treatment of 1 hour at 540^{o}C is sufficient to obtain a high level of properties in the T6 temper. A solution treatment of only 30 minutes caused the presence of brittle intermetallic phases due to an incomplete solution process. According to Dewhirst [12], the optimum solution treatment time at 540^{o}C is 4 hours. Birol [13] has recently investigated the effect of solution heat treatment on the age hardening capacity of dendritic and globular alloy F357. The DSC spectra of the dendritic and globular alloy were found to be nearly identical (Fig. 2.35). The peaks on Fig. 2.35 correspond to the following [13]:

1). Formation of clusters.

2). Dissolution of GP zones.

3). Precipitation of β″.

4). Formation of β′.

5). Precipitation of Si.

6). Formation of β.

Note that the DSC curves presented in Fig. 2.35 are for solution treated alloys, in contrast to the DSC curve in Fig. 2.33, which was for a T4 alloy. Fig. 2.35 therefore has a formation-of-clusters peak, whereas Fig. 2.33 has a relatively large dissolution-of clusters peak.

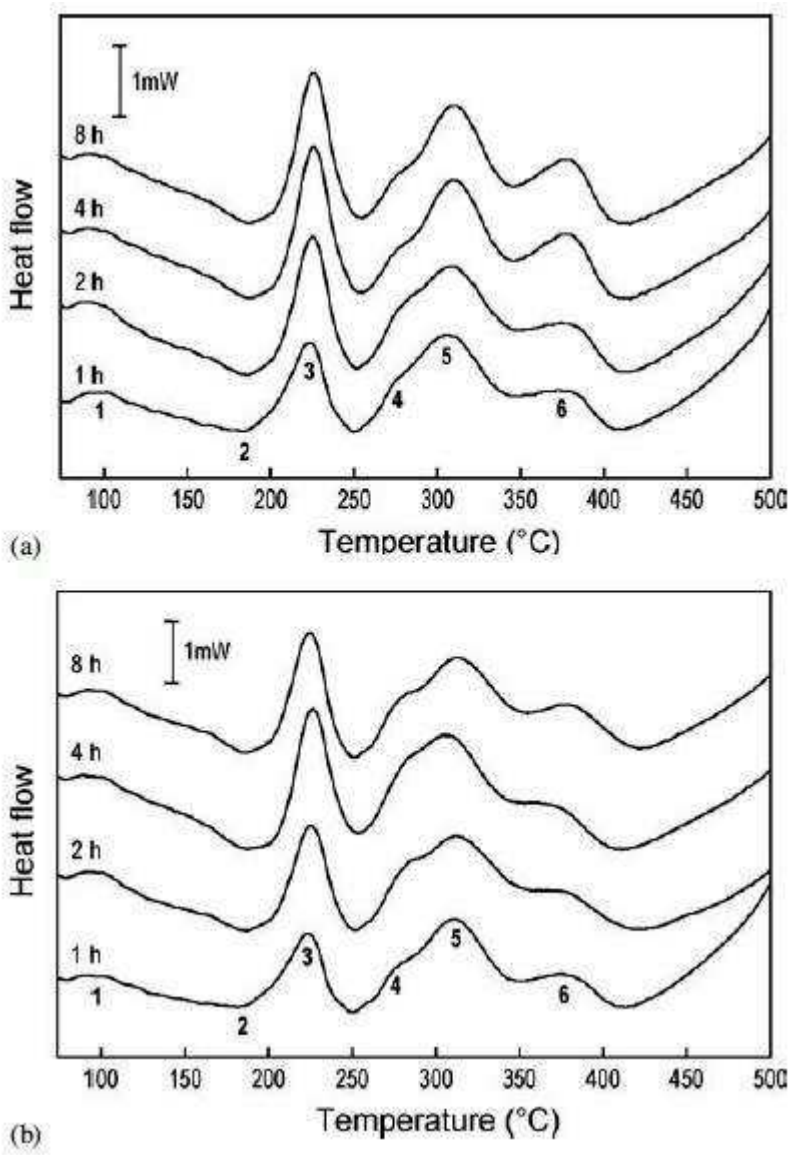

Figure 2.35: DSC scans of (a) dendritic and (b) globular F357 alloy after soaking at 540^{o}C for different times [13].

The response to artificial aging of the dendritic and globular alloys F357 which have been subjected to solution treatment at 540^{o}C for various times is illustrated in Fig. 2.36 [13]). The morphology of the primary α-Al, whether dendritic or globular, apparently has no effect on the artificial aging response of the alloy [13,14]. Birol [13] postulated that the favourable impact of the globular structure is offset by the relatively coarser structure in SSM-processed alloys. It is also seen from Fig. 2.36 that a solution treatment time of at least 2 h at 540^{o}C is required to obtain maximum hardness after artificial aging in this alloy.

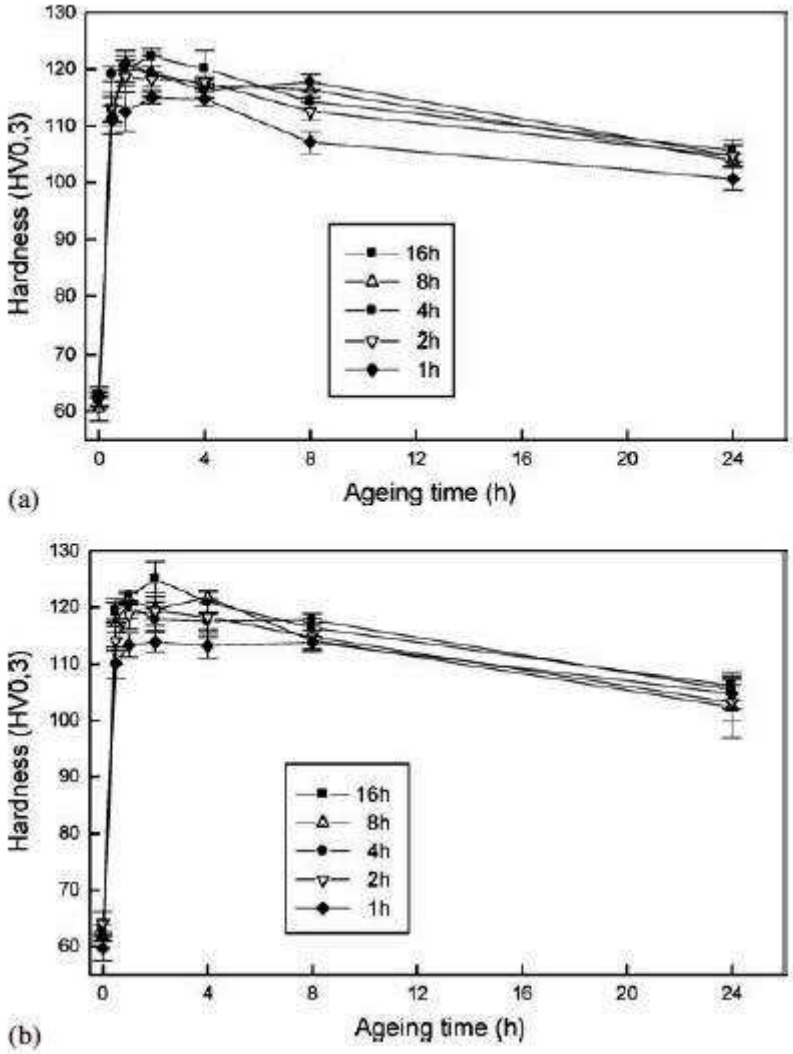

Figure 2.36: Artificial aging curves of (a) dendritic and (b) globular alloy F357 artificially aged at 190°C after solution treatment at 540°C for different times [13].

The influence of natural pre-aging on artificial aging has not received much attention when SSM processed Al-7Si-Mg alloys are heat treated to a T6 temper. According to Dewhirst [12], a natural aging time of eight hours is frequently used to ensure process uniformity. Dewhirst [12] varied the natural pre-aging time of semi-solid processed A356 between 8 and 24 hours and found that increasing the natural aging time beyond 8 hours had a slightly negative effect on the tensile properties of the material. However, it was concluded that artificial aging temperature and time were of much greater importance. Rosso and Actis Grande [90] also studied the optimisation of T6 heat treatment cycles for SSM-processed A356, but did not consider natural pre-aging time as a variable.

The artificial aging parameters of 170^{o}C for 6 hours are probably the most popular for SSM processed A356 [81,89,90]. There have been a few attempts to also shorten this treatment without compromising mechanical properties. Both Dewhirst [12] and Rosso and Actis Grande [90] determined the optimum artificial aging treatment for SSM processed A356 to be 4 h at 180^{o}C, with Birol [13,14] proposing 190^{o}C for 2 h for F357. The tensile properties for SSM-processed A356-T6 using the "traditional" heat treatment cycles, as well as the shorter cycles of 540^{o}C-1h and 180^{o}C-4h as proposed by Rosso and Actis Grande [90] are compared in Table 2.7.

Table 2.7: Brinell hardness (HB), yield strength (YS), UTS and %elongation of SSM-processed A356-T6 [90].

Heat treatment	HB	YS (MPa)	UTS (MPa)	%Elongation
Traditional	112	273	333	11
540^{o}C-1h; 180^{o}C-4h	113	279	332	10

The new, shorter cycles could lead to significant economic and environmental advantages. Temperature control (especially in the solution treatment step) and the performance and reliability of heat treating furnaces would then be of primary importance [90]. A summary of ASTM B969, the traditional and the proposed optimum heat treatment parameters for SSM-processed Al-7Si-Mg alloys is presented in Table 2.8.

Table 2.8: Summary of ASTM B969, the traditional and the proposed optimum heat treatment parameters for SSM-processed Al-7Si-Mg alloys.

	Solution heat treatment	Artificial aging
ASTM B969-10	540°C; 4-10h (A356) 540°C; 10h (A357)	160°C; 3-6h (A356) 170°C; 6h (A357)
"Traditional" [81,89]	540°C; 6h	170°C; 6h
Rosso and Actis Grande [90]	540°C; 1h (A356)	180°C; 4h (A356)
Dewhirst [12]	540°C; 4h (A356)	180°C; 4h (A356)
Birol [13,14]	540°C; 2h (F357)	190°C; 2h (F357)

Typical (or mid-range) mechanical properties for rheocast A356 and A357 in different temper conditions according to ASTM Standard B969-10 are listed in Table 2.9.

Table 2.9: Typical (or mid-range) mechanical properties for rheocast A356 and A357 in different temper conditions: ASTM B969-10.

Alloy	Temper	0.2% YS (MPa)	UTS	% Elongation in 5D
A356	F	110	240	11
	T5	180	270	6
	T6	235	310	11
A357	T6	290	345	6